PROCEEDINGS OF THE ROYAL SOCIETY B

rspb.royalsocietypublishing.org

Research

Cite this article: Louca S, Lampo M, Doebeli M. 2014 Assessing host extinction risk following exposure to *Batrachochytrium dendrobatidis*. *Proc. R. Soc. B* **281**: 20132783. http://dx.doi.org/10.1098/rspb.2013.2783

Received: 1 November 2013
Accepted: 2 April 2014

Subject Areas:
theoretical biology, health and disease and epidemiology, ecology

Keywords:
chytridiomycosis, invasion, extinction, epizootic, basic reproduction quotient

Author for correspondence:
Stilianos Louca
e-mail: stilianos.louca@gmail.com

Electronic supplementary material is available at http://dx.doi.org/10.1098/rspb.2013.2783 or via http://rspb.royalsocietypublishing.org.

Royal Society Publishing

Assessing host extinction risk following exposure to *Batrachochytrium dendrobatidis*

Stilianos Louca[1], Margarita Lampo[2] and Michael Doebeli[3,4]

[1]Institute of Applied Mathematics, University of British Columbia, 121-1984 Mathematics Road, Vancouver, British Columbia, Canada V6T 1Z2
[2]Centro de Ecología, Instituto Venezolano de Investigaciones Científicas, Apartado 21827, Caracas 1020-A, Venezuela
[3]Department of Zoology, and [4]Department of Mathematics, University of British Columbia, 6270 University Boulevard, Vancouver, British Columbia, Canada V6T 1Z4

Wildlife diseases are increasingly recognized as a major threat to biodiversity. Chytridiomycosis is an emerging infectious disease of amphibians caused by the fungus *Batrachochytrium dendrobatidis* (*Bd*). Using a mathematical model and simulations, we study its effects on a generic riparian host population with a tadpole and adult life stage. An analytical expression for the basic reproduction quotient, Q_o, of the pathogen is derived. By sampling the entire relevant parameter space, we perform a statistical assessment of the importance of all considered parameters in determining the risk of host extinction, upon exposure to *Bd*. We find that Q_o not only gives a condition for the initial invasion of the fungus, but is in fact the best predictor for host extinction. We also show that the role of tadpoles, which in some species tolerate infections, is ambivalent. While tolerant tadpoles may provide a reservoir for the fungus, thus facilitating its persistence or even amplifying its outbreaks, they can also act as a *rescue buffer* for a stressed host population. Our results have important implications for amphibian conservation efforts.

1. Introduction

Infectious wildlife diseases are linked to many recent animal population declines and are considered a major threat to biodiversity [1,2]. Understanding the dynamics of diseases and the factors that determine their long-term effects on host populations is an important step for conservation measures. Chytridiomycosis, an emerging infectious disease of amphibians [3], is caused by the fungus *Batrachochytrium dendrobatidis* (*Bd*) [4]. *Bd* has a wide host range and is now found on all continents where amphibians occur [5]. Its invasion can have devastating effects on host populations [6], and chytridiomycosis is currently linked to the decline or local extinction of over 200 amphibian species [7]. Nevertheless, many amphibian populations currently seem to be in a long-term endemic state with the fungus [8–10], often with a substantial reduction in survival [11].

The life cycle of *Bd* is a succession of a motile, waterborne, infectious zoospore and a substrate-bound thallus, the zoosporangium [12]. The zoospore encysts in a keratinized epidermal cell of its host [13] and transforms into a zoosporangium within a few days [14]. In the zoosporangium, new zoospores form, which are released towards the skin surface and into the external environment [15]. The exact pathophysiology of *Bd* is not fully understood, but disturbance of epidermal intercellular junctions seems to be involved in pathogenesis [16].

The prevalence of *Bd* and its effects on host populations have been statistically linked to abiotic conditions, such as temperature [17] and precipitation [18]. However, a complete mechanistic understanding of the interactions of demographic, immunological and environmental factors and their influence on the epizootic dynamics of *Bd* is lacking. Simple deterministic epizootic models with density-dependent transmission predict an eventual *fade out* of diseases, once the host population falls below a certain threshold. Recent findings, however, highlight

the role of tadpoles, which are less affected by infection than adults [19,20], as a potential reservoir facilitating the persistence of *Bd* [21], or even promoting host extinction [22]. Moreover, recent reports, suggesting the presence of *Bd* on aquatic birds [23] and crayfish [24], signify the risks of possible environmental reservoirs. It has also been theorized that a potentially long-lived free zoospore stage might contribute to local host extinctions [22,25,26].

Previous theoretical work on *Bd* by Mitchell *et al.* [22] and Briggs *et al.* [21] has succeeded in showing that all three scenarios, *Bd* clearance, *Bd*–host coexistence and host extinction, are possible epizootic outcomes even for the same host species. Mitchell *et al.* [22], however, neglect infected adults, do not consider within-host disease dynamics and ignore any possible variation in individual zoospore load. Keeping track of zoospore loads is important because (i) the progression of infection depends on reinfection events [12,17] and can vary greatly between individuals [27], (ii) zoospore load strongly influences pathogenesis [15,28] and (iii) the release of zoospores increases with fungal load [14]. Briggs *et al.* [21], on the other hand, assume that tadpoles are resistant to chytridiomycosis, a trait that may not be present in all frog species [20,29]. In addition, none of these models considers the possibility of seasonal variation of *Bd* transmission [30] and a possible regulation of on-host fungal growth (although its potential importance has been pointed out by Briggs *et al.*).

We propose a generic, continuous-time dynamical model for the interaction between *Bd* and an amphibian host population in an aquatic environment that addresses the above shortcomings of previous models. The host population includes two life stages, tadpoles and adults, and infections occur in both life stages through contact with zoospores in the water. Using analytical tools and numerical simulations, we investigate the short- and long-term consequences of an exposure of the host population to *Bd*. By systematically sampling the entire relevant parameter space, we assess the risk of host extinction as a function of the model parameters. We quantify the relative importance of model parameters using a dimensionless measure which we call *risk effect*. Finally, we investigate the role of the tadpoles in the epizootic and show that the host extinction risk need not necessarily increase when tadpoles tolerate infection (e.g. do not develop chytridiomycosis).

2. Material and methods

(a) Model description

In this section, we outline the epizootic model. A detailed description and justification of the model are provided in the electronic supplementary material, §1. We consider a single, closed, well-mixed amphibian population in a single aquatic habitat, interacting with a single *Bd* strain. The population is structured into two life stages, tadpoles and adults. Adults lay eggs at a constant or seasonally varying rate. Eggs quickly hatch as tadpoles and tadpoles metamorphose into adults at a constant rate. All newly recruited individuals are healthy. In the absence of *Bd*, the population is density regulated through competition, with adult and tadpole carrying capacities K_A and K_T, respectively.

The model keeps track of the distribution of the zoospore load, or *degree of infection* (DOI), across individuals. We denote by $P_A(t, n)$ and $P_T(t, n)$ the number of adults and tadpoles, respectively, that at time t are infected with $n \in 0, 1, \ldots$ zoospores, i.e. have DOI n. Because fungal load is usually estimated through the zoospore concentration on the host's skin [31], a zoospore-focused model allows for comparison with observations, as opposed to, say, a sporangium-focused model. We denote by $N_A(t) = \sum_{n=0}^{\infty} P_A(t, n)$ the total number of adults and by

$$S_A(t) = \frac{1}{N_A(t)} \sum_{n=0}^{\infty} n P_A(t, n)$$

the average DOI among all adults. $N_T(t)$ and $S_T(t)$ are defined in a similar way for tadpoles. The subscript s used hereafter for model parameters and variables, shall stand for either A (adults) or T (tadpoles).

New infections occur through contact with free zoospores released into the water by infected individuals [14]. This corresponds to findings suggesting that infested waters and sand might be the primary source of infection [21,28,32]. Infections might also change due to within-host disease dynamics, modelled through transition probability rates between DOIs. These transition rates depend on the exponential, within-host, disease growth or decay rates soon after exposure (λ_s), as well as the natural within-host zoospore loss rates ($\mu_{S,s}$).

The negative effects of *Bd* on the population are modelled by (i) an increased mortality rate of individuals, (ii) a decreased adult fecundity and (iii) a higher failure rate of metamorphoses [19,33]. The severity of all three effects increases with the DOI. For example, the yearly host survivorship is halved at a certain DOI *tolerance* level, $\mathcal{T}_s$ and the adult breeding rate is halved at a certain DOI, $\mathcal{T}_{br}$. Individuals die immediately if their DOI reaches a lethal threshold [28,32,34]. We also explicitly considered the case where tadpoles completely tolerate their infections, e.g. do not develop chytridiomycosis [19,20]. In that case, the tadpoles' DOI is nevertheless limited to a maximum possible value.

The model gives the temporal dynamics for the DOI distributions $P_A(t, n)$, $P_T(t, n)$ and the total number of free, active zoospores present in the water, the *zoospore pool* $Z(t)$. For the DOI distribution of adults, we have

$$\begin{aligned}\frac{d}{dt}P_A(t, n) = {} & [\beta_A(t)Z(t) + I_{A,u}(n-1)]P_A(t, n-1) \\ & + I_{A,d}(n+1)P_A(t, n+1) \\ & - [\beta_A(t)Z(t) + I_{A,u}(n) + I_{A,d}(n)]P_A(t, n) \\ & - [\mu_A(N_A(t)) + g_A(n)]P_A(t, n) \\ & + \frac{\delta_{n,0}}{\tau_m} \sum_{n'=0}^{\infty} \sigma_m(n')P_T(t, n'). \end{aligned} \tag{2.1}$$

The first three rows in (2.1) correspond to transitions between different DOIs. Here, $\beta_A(t)$ is the pool-to-adult *transmission rate*. It can be constant or annually oscillating, allowing us to investigate possible effects of seasonal variation. In our investigations, we varied its average value $\bar{\beta}_A$, its relative oscillation amplitude (b) and its phase lag (φ) with respect to the breeding season. The terms $I_{A,u}$, $I_{A,d}$ (*up* and *down*) represent transition rates between DOIs due to within-host dynamics. The fourth row corresponds to disease-independent and -dependent host mortality, the former increasing linearly with density. The last row describes the continuous metamorphosis of tadpoles into adults, at a rate $1/\tau_m$ and with a DOI-dependent probability of success $\sigma_m(n')$. The Kronecker delta $\delta_{n,0}$ is 1 if $n = 0$ and 0 otherwise, ensuring that new recruits are healthy. Similarly, for the tadpoles

$$\begin{aligned}\frac{d}{dt}P_T(t, n) = {} & [\beta_T(t)Z(t) + I_{T,u}(n-1)]P_T(t, n-1) \\ & + I_{T,d}(n+1)P_T(t, n+1) \\ & - [\beta_T(t)Z(t) + I_{T,u}(n) + I_{T,d}(n)]P_T(t, n) \\ & - \left[\mu_T(N_T(t)) + g_T(n) + \frac{1}{\tau_m}\right]P_T(t, n) \\ & + \delta_{n,0} r_{br}(t) \sum_{n'=0}^{\infty} \sigma_{br}(n')P_A(t, n'), \end{aligned} \tag{2.2}$$

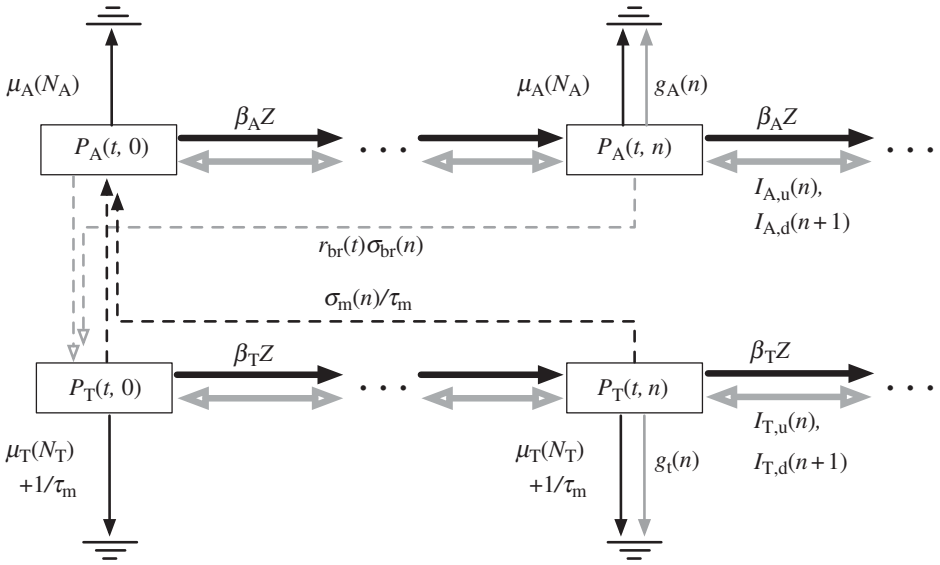

Figure 1. Schematic of the dynamics for the DOI distributions of adults (2.1) and tadpoles (2.2). Dashed arrows correspond to adult and tadpole recruitment, thin full arrows to disease-independent and disease-induced deaths, thick black arrows to new infections and thick grey arrows to within-host disease dynamics.

with the difference being the additional loss term $1/\tau_m$, which accounts for failed or successful metamorphoses. The breeding rate $r_{br}(t)$ can be constant or have an annual peak at the breeding season. We varied both the width of that peak (*breeding period*), as well as the overall scale of r_{br}, quantified by the cumulative *yearly fecundity*, $r = \int_0^{yr} r_{br}(t)\,dt$. The breeding rate is modulated by $\sigma_{br}(n')$, which mediates a possible DOI-dependent reduction in fecundity. See figure 1 for a schematic illustration of the dynamics (2.1) and (2.2). The dynamics of the zoospore pool are

$$\frac{dZ}{dt} = \sum_{s\in\{A,T\}} \eta_s N_s(t) S_s(t) - \mu_Z[Z(t) - Z_o].$$

Here, μ_Z is the *free zoospore loss rate* and η_s are the rates at which zoospores on hosts release new zoospores into the water. Z_o is the equilibrium size of a possible external zoospore pool in the absence of infected amphibians, referred to as *environmental reservoir*.

We note that one can derive mean field approximations of the dynamics (2.1) and (2.2), which are similar in structure to, but more general than the ones considered by May *et al.* [35, eqns (19,20)] (see the electronic supplementary material, §2.1). If the characteristic time scales of the zoospore pool are short compared with the epizootic dynamics [36, §6], we obtain a host-to-host transmission model similar to the one derived by Anderson *et al.* [37, eqn. (8)] (see the electronic supplementary material, §2.2). Important generalizations of our model, compared with [35,37], are the involvement of two host life stages and a seasonal variation of recruitment.

(b) Numerical simulations

The considered model parameter ranges for all simulations are given in table 1. Whenever possible, these ranges were chosen to roughly represent the values reported in the literature, or otherwise taken within plausible limits. Simulations typically ran for 10 years, and started with a healthy host population that was exposed to the pathogen during the second year.

We categorized each simulation outcome into one of the following three scenarios: (i) frog extinction, (ii) clearance of the fungus from the population and (iii) *Bd* persistence, i.e. the coexistence of the host and fungus in an endemic state by the end of the simulation. Using Monte Carlo simulations [38], we estimated the probability of any of the above scenarios, for varying values of each individual parameter, when all other parameters are randomly chosen from their entire range. We evaluated the effects of the different parameters on the probability of a disease-driven host extinction. We quantified the relative importance of each parameter by its so-called *risk effect*, which measures the change in the probability of host extinction, when the parameter is varied from its minimum to its maximum value. Risk effects were estimated through linear regression of the probability of extinction obtained from 10^4 trials (see the electronic supplementary material, §5.2).

We differentiated between cases where $Z_o = 0$ (no environmental reservoir) or $Z_o > 0$, and between cases where tadpoles suffer from infection or completely tolerate it. We also examined the effects of stochastic host demographics, by replacing the deterministic, disease-independent mortality in our simulations with random fatal events occurring at a constant Poissonian rate. This *stochastic model* is otherwise identical to the deterministic model described earlier. We refer to the electronic supplementary material, §5 for technical details.

3. Results and discussion

(a) Early invasion dynamics

Using a mean field approximation and standard linear stability theory [39], we analytically calculated the basic reproduction quotient Q_o of the fungus [40,41], introduced by Roberts *et al.* [36] for macroparasite models. Q_o (termed basic reproduction ratio, R_o, in Roberts *et al.*'s original formulation) has been defined as the number of adult parasites arising in the next generation from a single adult parasite, in a completely susceptible host population. It is comparable to the basic reproduction ratio in microparasite models [42]. Here, it gives the expected number of zoospores released into the water, originating from a single free zoospore, at the early stage of invasion in a newly exposed habitat. The condition $Q_o > 1$ is therefore a deterministic predictor for the successful invasion of *Bd*. We assumed that *Bd*-induced mortalities only become significant at a relatively high DOI and do not affect the early growth of the epizootic [3,34]. We refer to the electronic supplementary material, §2.3 for the derivation.

We find that the early epizootic dynamics strongly depend on (i) the exponential rate λ_s at which early infections

Table 1. Parameter ranges used in simulations. Exact parameter definitions are given in the electronic supplementary material, §1. Chosen values are justified in the electronic supplementary material, §5.1. All rates are in d^{-1}. Subscripts A and T refer to adults and tadpoles, respectively; the subscript s to either one. The case $\mathcal{F}_T = \infty$ corresponds to tadpoles tolerating their infection.

description	symbol	values
environmental reservoir	Z_o	0, $10-10^{15}$
free zoospore loss rate	μ_Z	$10^{-3}-1$
on-host zoospore loss rate	$\mu_{S,A}$	$10^{-3}-1$
on-host zoospore loss rate	$\mu_{S,T}$	$10^{-3}-1$
early infection growth rate	λ_A	$(-1)-1$
early infection growth rate	λ_T	$(-1)-1$
mean adult transmission rate	$\bar{\beta}_A$	$10^{-10}-10^{-3}$
mean tadpole transmission rate	$\bar{\beta}_T$	$10^{-10}-10^{-3}$
phase lag of transmission rates $\beta_s(t)$	φ	0–1 year
relative oscillation amplitude of $\beta_s(t)$	b	0–1
zoospore release rate	η_A	1–10
zoospore release rate	η_T	1–10
adult lethal DOI threshold	$\mathcal{F}_A$	10^4
tadpole lethal DOI threshold	$\mathcal{F}_T$	10^4, ∞
adult DOI tolerance	$\mathcal{T}_A$	$10-F_A$
tadpole DOI tolerance	$\mathcal{T}_T$	$10-F_T$
metamorphose DOI tolerance	$\mathcal{T}_m$	$10-10^6$
breeding DOI tolerance	$\mathcal{T}_{br}$	$10-10^6$
yearly adult fecundity	r	$10-10^3$
tadpole lifetime	τ_m	10 days to 4 years
breeding period	τ_{br}	1 day to 0.5 year
maximum adult survivorship	σ_A	0.1–0.9
maximum tadpole survivorship	σ_T	0.01–0.2
adult carrying capacity	K_A	$10-10^3$
tadpole carrying capacity	K_T	$10-10^3$

decay ($\lambda_s < 0$) or grow ($\lambda_s > 0$) within hosts, when excluding external reinfections and (ii) the time-averaged *per capita* recruitment (or turnover) rate $\bar{R}_s$ of each life stage s in the population prior to exposure. In particular, whenever $\lambda_s - \bar{R}_s \geq 0$ for at least one life stage s, the fungus will successfully invade upon exposure (in fact, in this case Q_o is formally infinite). But invasion is still possible, even if all $\lambda_s - \bar{R}_s < 0$. Then Q_o takes the form

$$Q_o = \frac{1}{\bar{\mu}_Z} \sum_{s \in \{A,T\}} \frac{\eta_s \bar{\beta}_s \bar{N}_s}{\bar{R}_s - \lambda_s}, \tag{3.1}$$

where $\bar{N}_s$ are the time-averaged population sizes in the uninfected community, $\bar{\mu}_Z$ is the time-averaged zoospore loss rate and $\bar{\beta}_s$ are the time-averaged transmission rates. The derivation of (3.1) assumes that the initial exposure is so weak and the resulting early *Bd* dynamics so slow that linear stability theory applies beyond the time scales over which the averaged variables change. In the alternative limit of rapid

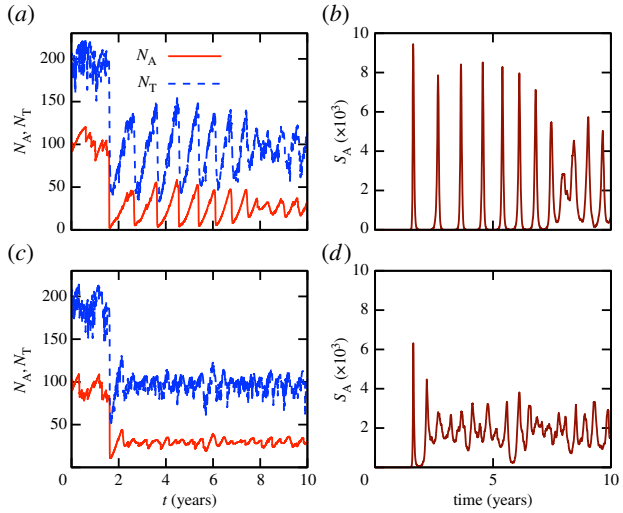

Figure 2. Simulations of the stochastic model (one per row), leading to endemic states. Panels (*a,c*) show population sizes, panels (*b,d*) show the mean adult DOI. The breeding rate r_{br} and transmission rates $\bar{\beta}_A$, $\bar{\beta}_T$ are time-independent. Populations are exposed to *Bd* during the second year. (*a,b*) Tadpoles do not suffer from infection and have a long life time ($\tau_m = 1$ year). The observed cycles are purely due to host-demographic delays, as *Bd*-intrinsic time scales are very short ($\mu_Z = 1\,d^{-1}$, $\mu_{S,A} = \mu_{S,T} = 0.2\,d^{-1}$). (*c,d*) Tadpoles strongly suffer from infection, but with otherwise identical parameters as in (*a,b*). Model parameters are given in the electronic supplementary material, table S1. (Online version in colour.)

Bd growth, all time averages should be replaced by their instantaneous values.

In fact, the above results, and in particular equation (3.1), hold for communities of multiple host species with multiple life stages and arbitrary recruitment flows and mortalities. The index s then runs through all species and life stages (see the electronic supplementary material, §2). Equation (3.1) highlights the increased risk of invasion associated with larger host population sizes. It also shows that the susceptibility of a single host species or life stage (i.e. for which $\lambda_s - \bar{R}_s \geq 0$) can jeopardize the entire community of a riparian habitat.

(b) Post-invasion dynamics

Simulations of the single-species model reproduce all three possible scenarios: (i) host extinction, (ii) clearance of the fungus from the population (or failure to invade) and (iii) long-term persistence of the fungus. All of these scenarios occur for a substantial parameter range, although by definition, clearance is only possible in the absence of an environmental reservoir ($Z_o = 0$).

Fungal persistence is typically accompanied by a permanent reduction of the host population to a fraction of its initial carrying capacity, as observed in numerous host–pathogen interactions and predicted by standard theory [43]. This reduction tends to be more severe as *Bd* transmission rates β_s or the reservoir Z_o increase. Figures 2*a–d* and 3*a* illustrate typical simulations resulting in long-term *Bd* persistence. Host population sizes increase during breeding periods (figure 3*a*), but can also vary due to epizootic cycles (figure 2*a*) or even due to stochastic mortalities. In fact, in many cases this stochasticity induces coherent cycles around an otherwise stable endemic state, a phenomenon known as quasi-cycles [44]. Furthermore, using cross-correlation

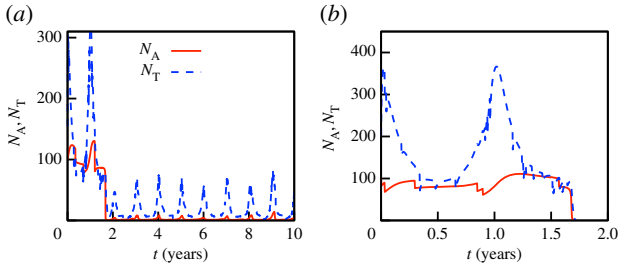

Figure 3. Adult population sizes during two similar simulations of the stochastic model. Annual peaks coincide with breeding seasons. The host population is exposed to the fungus during the second year. (*a*) Tadpoles do not suffer from infection and enable host survival, albeit at a reduced population size. (*b*) Tadpoles suffer from infection; all other parameters are identical to (*a*). Upon exposure to the fungus, the population quickly goes extinct. Model parameters are given in the electronic supplementary material, table S1. (Online version in colour.)

analysis [45, §14.2], we found that *Bd* prevalence positively correlates with recent host population sizes, usually with a delay that depends on the characteristic time scales of the epizootic (up to several months).

When host population sizes are low due to high *Bd* pressure, stochastic fluctuations can eventually cause host extinction [46]. But host extinction is also possible in the deterministic case, provided that *Bd* proliferation and host vulnerability are sufficiently high. Simple deterministic models of density-dependent disease transmission predict an eventual *fade out* of the pathogen, once the host population falls below a certain threshold [46]. However, if zoospores remain viable for a long time in lake water or sediments [25,26], then feedback delays in the density regulation of *Bd* proliferation can result in host extinction. Similar delays can appear if host recovery time scales exceed those of population crashes.

(c) Risk effects

The risk effects of the model parameters and Q_o are given in table 2. We note that even though Q_o is not an independent model parameter, its risk effect can still be defined and estimated (see the electronic supplementary material, §5.2).

Our results indicate that environmental reservoirs can have detrimental effects on host populations, and extinction becomes almost certain as their size (Z_o) exceeds a certain threshold. In the absence of environmental reservoirs ($Z_o = 0$), the two most important model parameters are the average transmission rate $\bar{\beta}_A$ and free zoospore loss rate μ_Z, in accordance with previous work [21,22]. Figure 4*a–d* shows the probabilities of host extinction, *Bd* prevalence and *Bd* clearance as functions of the tuple ($\bar{\beta}_A$, μ_Z). When $Z_o = 0$, all three parameter regions seem to be strongly determined by $\bar{\beta}_A$ and μ_Z, with the endemic regime separating regions favouring extinction (low μ_Z, high $\bar{\beta}_A$) from those favouring *Bd* clearance (high μ_Z, low $\bar{\beta}_A$). The negative risk effect of μ_Z underlines the risks associated with a potentially long-lived infectious zoospore, the existence of which still remains controversial [25,26,30]. We did not find significant risk effects for many of the other model parameters. For some of them, such as the zoospore release rates η_s, this was due to their relatively narrow ranges.

Interestingly, we found that the basic reproduction quotient Q_o shows the greatest predictive power for the extinction risk. The risk reaches 100% when Q_o exceeds a certain threshold, as seen in figure 5*a–d*. For $Z_o = 0$, *Bd* persistence becomes most likely at intermediate values $Q_o \approx 1$. Strictly speaking, Q_o only characterizes the early growth of the epizootic. Our results suggest that the efficiency of the fungus in proliferating at a site shortly after exposure strongly determines its long-term effect on host demographics. We point out that Q_o, as given by (3.1), is only valid if $\lambda_s - \bar{R}_s < 0$ for all host types. In the alternative case, Q_o is formally infinite and even though the fungus is expected to invade, our numerical results on its role in host extinction should not be extrapolated to these cases.

We emphasize that the risk effects calculated for the considered parameters, and therefore their order of importance, depend on their chosen ranges (table 1), more precisely on their true (unknown) probability distribution within those ranges. The resulting assessment should therefore be appreciated qualitatively. In special cases, the effect of certain parameters on the extinction risk might be stronger or even opposite to the predictions given here, as the latter are merely statistical and taken over a large parameter space. For example, in some cases we found that larger host carrying capacities actually increase the risk of extinction despite their negative risk effect, as they facilitate stronger epizootic outbreaks.

Table 2. Risk effects of model parameters and Q_o. Risk effects measure the direction and magnitude of change in the probability of host extinction, when a parameter is varied from its minimum to its maximum value. Only risk effects over 0.1 are shown; dash (—) represents lower values. Data columns 1 and 3: tadpoles suffer from infection. Data columns 2 and 4: tadpoles tolerate infection. Data columns 1 and 2: Z_o sampled from 10 to 10^{15}. Data columns 3 and 4: $Z_o = 0$. All model parameters were sampled in their entire range, given in table 1. Similar results were obtained for the stochastic model.

	$Z_o > 0$		$Z_o = 0$	
parameter	suffer	tolerate	suffer	tolerate
Q_o	+0.66	+0.83	+0.81	+0.71
Z_o	+0.66	+0.78	n.a.	n.a.
$\mathcal{T}_A$	−0.38	−0.47	−0.17	−0.28
μ_Z	−0.11	−0.20	−0.44	−0.46
$\bar{\beta}_A$	+0.32	+0.34	+0.38	+0.39
K_T	—	—	−0.27	−0.35
$\bar{\beta}_T$	+0.17	+0.27	+0.24	+0.18
$\mathcal{T}_T$	−0.24	n.a.	—	n.a.
K_A	—	—	−0.22	−0.12
λ_A	+0.17	+0.19	+0.18	+0.12
$\mu_{S,A}$	—	—	−0.14	−0.11
η_A	—	—	+0.13	—
$\mu_{S,T}$	—	—	—	−0.12
$\mathcal{T}_{br}$	—	—	—	−0.10

(d) The role of tadpoles

As adult densities decrease, tadpoles can act as a temporary reservoir for *Bd*, if they can tolerate infection and remain in the tadpole stage for long times. This effect can lead to

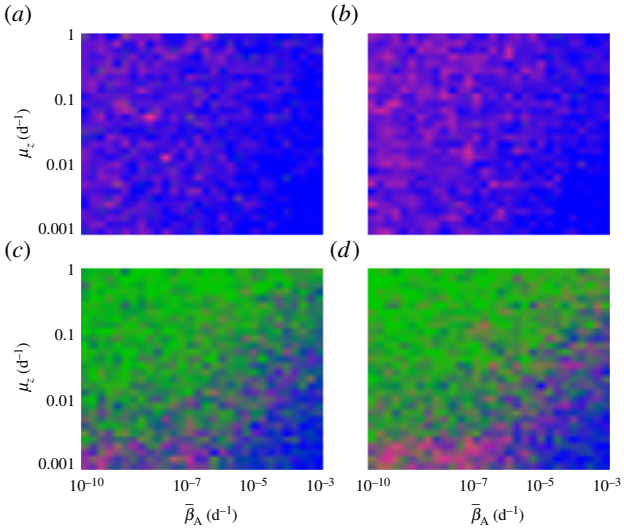

Figure 4. Estimated probabilities of *Bd* persistence, *Bd* clearance and host extinction, as functions of $\bar{\beta}_A$ and μ_Z in the deterministic model, shown as colour codes. Pure colours green, magenta and blue correspond to 100% *Bd* clearance, *Bd* persistence and host extinction, respectively. Mixed probabilities appear as compound colours. (*a,b*) $Z_o > 0$. (*c,d*) $Z_o = 0$. (*a,c*) Tadpoles suffer from infection. (*b,d*) Tadpoles tolerate *Bd*. All other model parameters were sampled within their entire range, as described in the electronic supplementary material, §5.2. Similar results were obtained for the stochastic model.

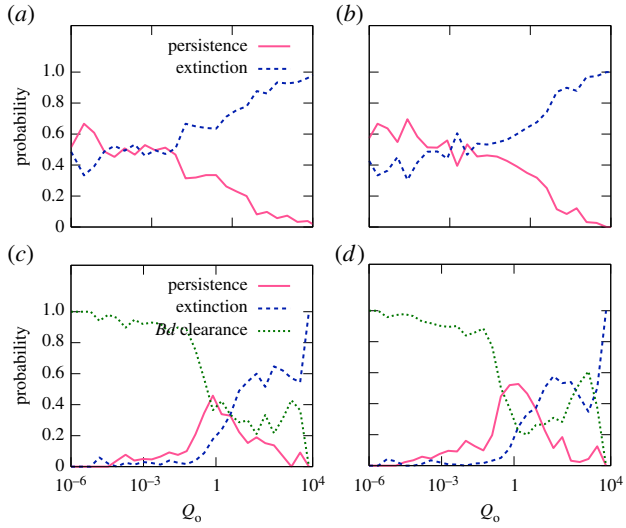

Figure 5. Estimated probabilities of *Bd* persistence, *Bd* clearance and host extinction in the deterministic model, as functions of the basic reproduction quotient, Q_o. (*a,b*) The environmental reservoir Z_o ranges from 10 to 10^{15} zoospores. (*c,d*) No reservoir ($Z_o = 0$). (*a,c*) Tadpoles suffer from infection. (*b,d*) Tadpoles tolerate infection. All other model parameters were sampled within their entire range. Similar results were obtained for the stochastic model. (Online version in colour.)

strong *Bd* outbreaks and host population declines, even when zoospore death and within-host clearance rates are high ($\mu_Z \approx 1\,d^{-1}$, $\mu_{S,s} \gtrsim 0.2\,d^{-1}$). Shorter tadpole stages dampen these outbreaks, but *Bd* prevalence is still generally higher and adult densities lower when tadpoles tolerate *Bd*, compared with when they do not. These observations are exemplified by simulations shown in figure 2*a–d*. In figure 2*a,b*, a long tadpole stage and *Bd* tolerance lead to strong outbreaks and fluctuations in host densities. An increased *Bd*-induced tadpole mortality dampens these outbreaks, as demonstrated by the simulations in figure 2*c,d*. Adult population sizes are greatest when tadpoles suffer from *Bd* and the tadpole stage is short. These findings are supported by observations linking longer tadpole stages and decreased tadpole vulnerability to increased *Bd* prevalence [19,47].

In the presence of environmental reservoirs ($Z_o > 0$), or for long zoospore life expectancies within and outside of hosts ($\gtrsim 10$ days), the significance of tadpoles as a reservoir diminishes. The fungus then persists even when tadpoles suffer from infection and the overall host mortality becomes important. The negative risk effect of the tadpole carrying capacity K_T (table 2), which is particularly strong when tadpoles completely tolerate infection, suggests that tolerant tadpoles act as a rescue buffer during strong outbreaks. Figure 3*a,b* exemplifies this idea. It shows two similar simulations in which tadpoles either tolerate infection (*a*) or suffer from it (*b*), with extinction only occurring in the latter case. When sampling over the entire parameter space (with $Z_o = 0$), we observed a slightly increased fraction of host extinctions (25%) when tadpoles suffer from infection, compared with cases where tadpoles tolerate *Bd* (only 21% extinctions).

Our findings underline the complex role of the tadpole–adult life cycle in the epizootic [19]. We tested the robustness of these results against a variation in the way this life cycle is modelled. We investigated an alternative model, in which tadpoles attempt metamorphosis once they reach a certain age τ_m, but not before. Such a delayed metamorphosis is in contrast to our original model, in which tadpoles metamorphose at a constant rate right from the start of their life as tadpole. All other aspects of our original model are kept identical, allowing a cross-comparison of the two schemes. We refer to the electronic supplementary material, §3 for details. Simulations generally showed behaviour that was qualitatively similar to our original model. However, the parameter space for which the host population persists for longer times (even in the absence of disease) is somewhat smaller. This is because the prolonged tadpole stage exposes tadpoles to a higher cumulative risk of death and tends to destabilize dynamics. Nevertheless, this alternative model reproduces the reported ambivalent role of tadpoles, depending on their susceptibility and life time as well as the zoospore loss rate.

4. Conclusion

We have investigated the short- and long-term demographic effects of *Bd* on an exposed host population, using a generic, mechanistic mathematical model that includes various possible host–pathogen interactions. Our statistical assessment provides a rank of importance for several epizootic, immunological and demographic parameters with respect to their influence on the risk of extinction. Our approach can be seen as an alternative to conventional elasticity analysis [48] as well as regression methods used in sensitivity analysis [49,50]. Both theories aim at estimating the importance of demographic parameters for population growth and extinction risk. A novelty of our approach is the systematic evaluation of the entire 25-dimensional parameter space, which was able to reveal relationships between focal parameters and the epizootic dynamics, independently of a particular choice of the other

parameters. Moreover, the population viability analysis given here [51] can easily be adapted to virtually any wildlife disease model that includes host demographics [36].

The transmission rates $\bar{\beta}_s$, zoospore loss rates μ_Z, $\mu_{S,s}$ and immunological parameters such as λ_s and $\mathcal{T}_s$, are strongly linked to abiotic factors like temperature and pH [4,14,30]. A better understanding of these links will provide a connection between our parametrization and site-specific abiotic factors. This will enable a possible translation of our results, or at least methodology, to an explicit risk assessment for the numerous amphibian species threatened by the fungus. However, for accurate site- and species-specific predictions, further details are required on *Bd* physiology and the interaction with its hosts, in order to narrow down the parameter ranges to be considered. In table 2, we have provided a suggested priority list of parameters expected to be of particular importance.

The strong predictive power of Q_o for host extinction, as found by our simulations, suggests that the efficiency of the fungus in proliferating at a site shortly after exposure strongly determines its long-term effects on host demographics. Rapid epizootic growth during the invasion phase should therefore be seen as a strong warning signal for a possible imminent local extinction. Thus, estimating Q_o for individual sites holds great potential for prioritizing future conservation efforts.

We showed that the effect of tolerant tadpoles on host extinction risk is ambivalent, and depends on the loss rate of zoospores within and outside of hosts. Our results complement prevailing, but simplistic views of tolerant tadpoles contributing to stronger outbreaks and facilitating *Bd* persistence [19–21].

We emphasize that if more than one host species are involved, the epizootic dynamics are likely to be more complicated [52]. In fact, in that case a tolerant species acting as a reservoir could induce the extinction of another more susceptible coexisting species [19,53]. Our derivation of the basic reproduction quotient, Q_o, in multi-species communities (§3.1) is a small step towards the theoretical understanding of the expected dynamics.

Acknowledgement. We thank Angie Nicolás for her valuable suggestions.
Funding statement. This work was supported by the PIMS IGTC for Mathematical Biology and NSERC (Canada).

References

1. Daszak P, Cunningham AA, Hyatt AD. 2000 Emerging infectious diseases of wildlife—threats to biodiversity and human health. *Science* **287**, 443–449. (doi:10.1126/science.287.5452.443)
2. Smith K, Acevedo-Whitehouse K, Pedersen A. 2009 The role of infectious diseases in biological conservation. *Anim. Conserv.* **12**, 1–12. (doi:10.1111/j.1469-1795.2008.00228.x)
3. Kilpatrick AM, Briggs CJ, Daszak P. 2010 The ecology and impact of chytridiomycosis: an emerging disease of amphibians. *Trends Ecol. Evol.* **25**, 109–118. (doi:10.1016/j.tree.2009.07.011)
4. Longcore JE, Pessier AP, Nichols DK. 1999 *Batrachochytrium dendrobatidis* gen. et sp. nov., a chytrid pathogenic to amphibians. *Mycologia* **91**, 219–227. (doi:10.2307/3761366)
5. Fisher MC, Garner TW, Walker SF. 2009 Global emergence of *Batrachochytrium dendrobatidis* and amphibian chytridiomycosis in space, time, and host. *Annu. Rev. Microbiol.* **63**, 291–310. (doi:10.1146/annurev.micro.091208.073435)
6. Lips KR *et al*. 2006 Emerging infectious disease and the loss of biodiversity in a Neotropical amphibian community. *Proc. Natl Acad. Sci. USA* **103**, 3165–3170. (doi:10.1073/pnas.0506889103)
7. Skerratt LF, Berger L, Speare R, Cashins S, McDonald KR, Phillott AD, Hines HB, Kenyon N. 2007 Spread of chytridiomycosis has caused the rapid global decline and extinction of frogs. *Eco Health* **4**, 125–134. (doi:10.1007/s10393-007-0093-5)
8. Retallick RW, McCallum H, Speare R. 2004 Endemic infection of the amphibian chytrid fungus in a frog community post-decline. *PLoS Biol.* **2**, e351. (doi:10.1371/journal.pbio.0020351)
9. Lampo M *et al*. 2008 *Batra-chochytrium dendrobatidis* in Venezuela. *Herpetol. Rev.* **39**, 449.
10. Lampo M, Celsa SJ, Rodríguez-Contreras A, Rojas-Runjaic F, García CZ. 2012 High turnover rates in remnant populations of the harlequin frog *Atelopus cruciger* (*Bufonidae*): low risk of extinction? *Biotropica* **44**, 420–426. (doi:10.1111/j.1744-7429.2011.00830.x)
11. Murray KA, Skerratt LF, Speare R, Mc-Callum H. 2009 Impact and dynamics of disease in species threatened by the amphibian chytrid fungus, *Batrachochytrium dendrobatidis*. *Conserv. Biol.* **23**, 1242–1252. (doi:10.1111/j.1523-1739.2009.01211.x)
12. Berger L, Hyatt AD, Speare R, Longcore JE. 2005 Life cycle stages of the amphibian chytrid *Batrachochytrium dendrobatidis*. *Dis. Aquat. Org.* **68**, 51–63. (doi:10.3354/dao068051)
13. Pessier AP, Nichols DK, Longcore JE, Fuller MS. 1999 Cutaneous chytridiomycosis in poison dart frogs (*Dendrobates* spp.) and White's tree frogs (*Litoria caerulea*). *J. Vet. Diagn. Invest.* **11**, 194–199. (doi:10.1177/104063879901100219)
14. Woodhams DC, Alford RA, Briggs CJ, Johnson M, Rollins-Smith LA. 2008 Lifehistory trade-offs influence disease in changing climates: strategies of an amphibian pathogen. *Ecology* **89**, 1627–1639. (doi:10.1890/06-1842.1)
15. Voyles J, Rosenblum EB, Berger L. 2011 Interactions between *Batrachochytrium dendrobatidis* and its amphibian hosts: a review of pathogenesis and immunity. *Microbes Infect.* **13**, 25–32. (doi:10.1016/j.micinf.2010.09.015)
16. Brutyn M *et al*. 2012 *Batrachochytrium dendrobatidis* zoospore secretions rapidly disturb intercellular junctions in frog skin. *Fungal Genet. Biol.* **49**, 830–837. (doi:10.1016/j.fgb.2012.07.002)
17. Forrest MJ, Schlaepfer MA. 2011 Nothing a hot bath won't cure: infection rates of amphibian chytrid fungus correlate negatively with water temperature under natural field settings. *PLoS ONE* **6**, e28444. (doi:10.1371/journal.pone.0028444)
18. Murray KA, Retallick RWR, Puschendorf R, Skerratt LF, Rosauer D, McCallum HI, Berger L, Speare R, VanDerWal J. 2011 Assessing spatial patterns of disease risk to biodiversity: implications for the management of the amphibian pathogen, *Batrachochytrium dendrobatidis*. *J. Appl. Ecol.* **48**, 163–173. (doi:10.1111/j.1365-2664.2010.01890.x)
19. Rachowicz LJ *et al*. 2004 Transmission of *Batrachochytrium dendrobatidis* within and between amphibian life stages. *Dis. Aquat. Org.* **61**, 75–83. (doi:10.3354/dao061075)
20. Blaustein AR, Romansic JM, Scheessele EA, Han BA, Pessier AP, Longcore JE. 2005 Interspecific variation in susceptibility of frog tadpoles to the pathogenic fungus *Batrachochytrium dendrobatidis*. *Conserv. Biol.* **19**, 1460–1468. (doi:10.1111/j.1523-1739.2005.00195.x)
21. Briggs CJ, Knapp RA, Vredenburg VT. 2010 Enzootic and epizootic dynamics of the chytrid fungal pathogen of amphibians. *Proc. Natl Acad. Sci. USA* **107**, 9695–9700. (doi:10.1073/pnas.0912886107)
22. Mitchell KM, Churcher TS, Garner TW, Fisher MC. 2008 Persistence of the emerging pathogen *Batrachochytrium dendrobatidis* outside the amphibian host greatly increases the probability of host extinction. *Proc. R. Soc. B* **275**, 329–334. (doi:10.1098/rspb.2007.1356)
23. Garmyn A, Van Rooij P, Pasmans F, Hellebuyck T, Van Den Broeck W, Haesebrouck F, Martel A. 2012 Waterfowl: potential environmental reservoirs of

the chytrid fungus *Batrachochytrium dendrobatidis*. *PLoS ONE* **7**, e35038. (doi:10.1371/journal.pone.0035038)

24. McMahon TA *et al*. 2013 Chytrid fungus *Batrachochytrium dendrobatidis* has nonamphibian hosts and releases chemicals that cause pathology in the absence of infection. *Proc. Natl Acad. Sci. USA* **110**, 210–215. (doi:10.1073/pnas.1200592110)
25. Johnson ML, Speare R. 2003 Survival of *Batrachochytrium dendrobatidis* in water: quarantine and disease control implications. *Emerg. Infect. Dis.* **9**, 922. (doi:10.3201/eid0908.030145)
26. Johnson ML *et al*. 2005 Possible modes of dissemination of the amphibian chytrid *Batrachochytrium dendrobatidis* in the environment. *Dis. Aquat. Org.* **65**, 181–186. (doi:10.3354/dao065181)
27. Berger L, Speare R, Skerratt LF. 2005 Distribution of *Batrachochytrium dendrobatidis* and pathology in the skin of green tree frogs *Litoria caerulea* with severe chytridiomycosis. *Dis. Aquat. Org.* **68**, 65–70. (doi:10.3354/dao068065)
28. Carey C, Bruzgul JE, Livo LJ, Walling ML, Kuehl KA, Dixon BF, Pessier AP, Alford RA, Rogers KB. 2006 Experimental exposures of boreal toads (*Bufo boreas*) to a pathogenic chytrid fungus (*Batrachochytrium dendrobatidis*). *Eco Health* **3**, 5–21. (doi:10.1007/s10393-005-0006-4)
29. Venesky MD, Parris MJ, Storfer A. 2009 Impacts of *Batrachochytrium dendrobatidis* infection on tadpole foraging performance. *Eco Health* **6**, 565–575. (doi:10.1007/s10393-009-0272-7)
30. Piotrowski JS, Annis SL, Longcore JE. 2004 Physiology of *Batrachochytrium dendrobatidis*, a chytrid pathogen of amphibians. *Mycologia* **96**, 9–15. (doi:10.2307/3761981)
31. Hyatt A *et al*. 2007 Diagnostic assays and sampling protocols for the detection of *Batrachochytrium dendrobatidis*. *Dis. Aquat. Org.* **73**, 175–192. (doi:10.3354/dao073175)
32. Cashins SD, Grogan LF, McFadden M, Hunter D, Harlow PS, Berger L, Skerratt LF. 2013 Prior infection does not improve survival against the amphibian disease chytridiomycosis. *PLoS ONE* **8**, e56747. (doi:10.1371/journal.pone.0056747)
33. Garner TW, Walker S, Bosch J, Leech S, Rowcliffe JM, Cunningham AA, Fisher MC. 2009 Life history tradeoffs influence mortality associated with the amphibian pathogen *Batrachochytrium dendrobatidis*. *Oikos* **118**, 783–791. (doi:10.1111/j.1600-0706.2008.17202.x)
34. Stockwell MP, Clulow J, Mahony MJ. 2010 Host species determines whether infection load increases beyond disease-causing thresholds following exposure to the amphibian chytrid fungus. *Anim. Conserv.* **13**, 62–71. (doi:10.1111/j.1469-1795.2010.00407.x)
35. May RM, Anderson RM. 1978 Regulation and stability of host-parasite population interactions: II. Destabilizing processes. *J. Anim. Ecol.* **47**, 249–267. (doi:10.2307/3934)
36. Roberts MG, Smith G, Grenfell BT. 1995 Mathematical models for macroparasites of wildlife. In *Ecology of infectious diseases in natural populations* (eds BT Grenfell, AP Dobson), *Publications of the Newton Institute*, no. 7, pp. 177–208. Cambridge, UK: Cambridge University Press.
37. Anderson RM, May RM. 1978 Regulation and stability of host–parasite population interactions: I. Regulatory processes. *J. Anim. Ecol.* **47**, 219–247. (doi:10.2307/3933)
38. Hammersley JM, Handscomb DC. 1964 *Monte Carlo methods*. London, UK: Methuen.
39. Michel A, Hou L, Liu D. 2008 *Stability of dynamical systems: continuous, discontinuous, and discrete systems*. Boston, MA: Systems & Control Birkhäuser.
40. Roberts M. 1995 A pocket guide to host–parasite models. *Parasitol. Today* **11**, 172–177. (doi:10.1016/0169-4758(95)80150-2)
41. Heesterbeek J, Roberts M. 1995 Threshold quantities for helminth infections. *J. Math. Biol.* **33**, 415–434. (doi:10.1007/BF00176380)
42. Heesterbeek J, Dietz K. 1996 The concept of R_0 in epidemic theory. *Stat. Neerl.* **50**, 89–110. (doi:10.1111/j.1467-9574.1996.tb01482.x)
43. Anderson RM, May RM. 1981 The population dynamics of microparasites and their invertebrate hosts. *Phil. Trans. R. Soc. Lond. B* **291**, 451–524. (doi:10.1098/rstb.1981.0005)
44. Pineda-Krch M, Blok H, Dieckmann U, Doebeli M. 2007 A tale of two cycles – distinguishing quasi-cycles and limit cycles in finite predator–prey populations. *Oikos* **116**, 53–64. (doi:10.1111/j.2006.0030-1299.14940.x)
45. Wei W. 2005 *Time series analysis: univariate and multivariate methods*, 2nd edn. Reading, MA: Addison Wesley.
46. De Castro F, Bolker B. 2005 Mechanisms of disease-induced extinction. *Ecol. Lett.* **8**, 117–126. (doi:10.1111/j.1461-0248.2004.00693.x)
47. Bosch J, Martínez-Solano I, García-París M. 2001 Evidence of a chytrid fungus infection involved in the decline of the common midwife toad (*Alytes obstetricans*) in protected areas of central Spain. *Biol. Conserv.* **97**, 331–337. (doi:10.1016/S0006-3207(00)00132-4)
48. de Kroon H, van Groenendael J, Ehrlén J. 2000 Elasticities: a review of methods and model limitations. *Ecology* **81**, 607–618. (doi:10.1890/0012-9658(2000)081[0607:EAROMA]2.0.CO;2)
49. McCarthy MA, Burgman MA, Ferson S. 1995 Sensitivity analysis for models of population viability. *Biol. Conserv.* **73**, 93–100. (doi:10.1016/0006-3207(95)90029-2)
50. Cariboni J, Gatelli D, Liska R, Saltelli A. 2007 The role of sensitivity analysis in ecological modelling. *Ecol. Model.* **203**, 167–182. (doi:10.1016/j.ecolmodel.2005.10.045)
51. Gerber LR, McCallum H, Lafferty KD, Sabo JL, Dobson A. 2005 Exposing extinction risk analysis to pathogens: is disease just another form of density dependence? *Ecol. Appl.* **15**, 1402–1414. (doi:10.1890/04-0880)
52. Searle CL, Biga LM, Spatafora JW, Blaustein AR. 2011 A dilution effect in the emerging amphibian pathogen *Batrachochytrium dendrobatidis*. *Proc. Natl Acad. Sci. USA* **108**, 16 322–16 326. (doi:10.1073/pnas.1108490108)
53. Daszak P, Strieby A, Cunningham AA, Longcore J, Brown C, Porter D. 2004 Experimental evidence that the bullfrog (*Rana catesbeiana*) is a potential carrier of chytridiomycosis, an emerging fungal disease of amphibians. *Herpetol. J.* **14**, 201–207.

Supplementary material to article

Assessing host extinction risk following exposure to *Batrachochytrium dendrobatidis*

Stilianos Louca, Margarita Lampo, Michael Doebeli

March 31, 2014

Abstract

This document is supplementary to the main article. We provide proofs of our mathematical results, justification of the models and parameter ranges, as well as minor extensions of our work not given in the main article.

1 Elaborations on the single species model

Here, we describe in detail the single-species model introduced in section 2.1 of the main article and used in our simulations.

1.1 Breeding

We assume that adults mate and lay eggs throughout the year at a rate proportional to a time-dependent breeding function $r_{\mathrm{br}}(t)$, modulated by a factor $\sigma_{\mathrm{br}}(n)$ that decreases with the DOI n and satisfies $\sigma_{\mathrm{br}}(0) = 1$. The latter represents possible negative effects of infections on adult fecundities. We assume eggs to hatch in a time so short that it can be neglected, so that $r_{\mathrm{br}}(t) \sum_n \sigma_{\mathrm{br}}(n) P_{\mathrm{A}}(t,n)$ gives the current tadpole recruitment rate. We refer to the yearly number of hatched tadpoles per healthy adult, $r := \int_0^Y r_{\mathrm{br}}(t)\ dt$ (where Y is the duration of one year), as yearly host fecundity. The specific function $r_{\mathrm{br}}(t)$ and modulating factor $\sigma_{\mathrm{br}}(n)$ used in our simulations are given in section 1.4. $r_{\mathrm{br}}(t)$ exhibits a yearly minimum and maximum (breeding period) at equal intervals, reflecting seasonal variation of recruitment rates [1]. It is parameterized by the yearly fecundity r and its Full-Width-at-Half-Maximum (FWHM), τ_{br}, which is a measure for the length of each breeding period. $\sigma_{\mathrm{br}}(n)$ is parameterized by the breeding tolerance $\mathcal{T}_{\mathrm{br}}$, which gives the DOI for which $\sigma_{\mathrm{br}}(\mathcal{T}_{\mathrm{br}}) = 1/2$.

Tadpoles attempt metamorphosis regardless of age and DOI at a rate $1/\tau_{\mathrm{m}}$, where $\tau_{\mathrm{m}} > 0$ is the expected tadpole lifetime. Metamorphosis of a tadpole with DOI $n \geq 0$ succeeds with probability $\sigma_{\mathrm{m}}(n) \in (0,1]$, and results in death otherwise. Newly hatched tadpoles, as well as recently metamorphosed adults, are assumed to be healthy. Alternatively, one might assume that metamorphosis succeeds with probability $\sigma_{\mathrm{m}}(0)$, resulting in a non-infected adult. The latter then quickly dies with probability $1 - \sigma_{\mathrm{m}}(n)/\sigma_{\mathrm{m}}(0)$ due to after-effects of its *Bd* infection [2, 3, 4]. The exact functional response $\sigma_{\mathrm{m}}(n)$, which decreases for increasing n, is given in section 1.4. It is parameterized by the so called metamorphosing tolerance $\mathcal{T}_{\mathrm{m}}$, which gives the DOI for which $\sigma_{\mathrm{m}}(\mathcal{T}_{\mathrm{m}}) = \sigma_{\mathrm{m}}(0)/2$. Thus, a lower $\mathcal{T}_{\mathrm{m}}$ corresponds to a greater impact of *Bd* on metamorphosis.

1.2 Host mortalities

In the absence of disease, we model adult death by a per-capita mortality rate $\mu_{\mathrm{A}}(\mathbf{N})$, which depends on the current population state $\mathbf{N}$. The so called base survivorship $\sigma_{\mathrm{A}} := e^{-Y\mu_{\mathrm{A}}(0)}$ gives the yearly survival probability of healthy adults, in the absence of any density effects (e.g. subject only to random disturbances and predation). Let $\mu_{\mathrm{T}}(\mathbf{N})$ and σ_{T} be defined in a similar way for tadpoles. The negative effects of a DOI n on adults, are reflected in a further increase of the mortality rate by an additive factor $g_{\mathrm{A}}(n)$, which increases with the DOI n. Similarly, the mortality rate for tadpoles of DOI n is given by $\mu_{\mathrm{T}}(\mathbf{N}) + g_{\mathrm{T}}(n)$. The specific form for μ_{A} and μ_{T} used in our simulations, is given in section 1.4. We parameterize the mortalities using the base survivorships σ_s and the carrying capacities K_{A}, K_{T}, an approximation for the average population sizes in the absence of disease. See section 1.5 for details.

The functional responses $g_s(n)$ (where $s \in \{\mathrm{A}, \mathrm{T}\}$) of mortality to infection are highly species- and life-stage specific [5, 3, 6, 7, 8, 9]. Recent findings indicate the existence of thresholds for the maximum infection load that certain species can tolerate [10, 7, 11, 12], although continuous dependencies of mortality on the DOI have also been observed [10, 13]. For our simulations, we thus parameterize g_s by the lethal DOI $\mathcal{F}_s$, which satisfies $g_s(\mathcal{F}_s) = \infty$, and the so called host tolerance $\mathcal{T}_s$, which

gives the DOI at which the yearly survivorship of an infected individual is reduced by a factor 2, compared to a healthy one.

1.3 Disease dynamics

In our model, we assume autonomous, i.e., time independent within-host dynamics of the infection. Concretely, in the absence of external secondary infections, the DOI of an infected individual at life stage $s \in \{\mathrm{A}, \mathrm{T}\}$ may increase from n to $n+1$ at a probability rate $I_{s,\mathrm{u}}(n)$, and decrease from n to $n-1$ at a probability rate $I_{s,\mathrm{d}}(n)$. We point out that the processes underlying the two types of transitions can be fundamentally different. Furthermore, this Markovian (i.e., memoryless) description presumes the absence of an adaptive immune response, as suggested by recent findings for certain species [14, 12]. It also ignores possible time-delays of the host's innate immune reaction [15, 16, 17] and long-term effects of disease-induced physiological stress. Nevertheless, it is adequate for differentiating between an efficient and inefficient innate immune response [18, 7], as well as between colonial growth and slow decay of the infection if, for example, tubes completely discharge to the external environment [19]. Note that $I_s(n) := I_{s,\mathrm{u}}(n) - I_{s,\mathrm{d}}(n)$ gives the *expected* DOI growth speed of an infected individual having DOI n.

In section 1.4 we elaborate on the specific form of $I_{s,\mathrm{u}}$ and $I_{s,\mathrm{d}}$, which we parameterize by the early within-host growth rate $\lambda_s := I_s'(0)$ (which can be positive or negative) and the asymptotic decay rate $\mu_{\mathrm{S},s} := \lim_{n\to\infty} - I_s(n)/n$. The latter is also the intrinsic within-host zoospore loss rate. We introduce an upper bound, $S_{\mathrm{T,max}}$, for the maximum DOI a tadpole can possibly have. We either take $S_{\mathrm{T,max}} = \mathcal{F}_\mathrm{T}$ with $\mathcal{T}_\mathrm{T} < \mathcal{F}_\mathrm{T}$ or $S_{\mathrm{T,max}} = \mathcal{F}_\mathrm{T} - 1$ with $\mathcal{T}_\mathrm{T} = \mathcal{F}_\mathrm{T}$. In the second case tadpoles get infected but *tolerate* their infections, i.e. do not suffer an increased mortality, corresponding to observations in certain species [2, 5].

Recent findings suggest that the primary source of infection might be zoospore-infested waters and sand [10, 20, 12], and *Bd* prevalence has been found to increase more rapidly in riparian than surrounding terrestrial habitats in Panama [21]. We thus ignore direct-contact transmission and assume (primary or secondary) infections to occur at a rate $\beta_s(t)Z(t)N(t)$, the *force of infection*. The Y-periodic transmission rate $\beta_s(t)$ can be seen as the probability rate at which a free zoospore is encountered by a particular host at stage $s \in \{\mathrm{A}, \mathrm{T}\}$, multiplied by the probability that such an encounter might lead to a successful infection [22]. The seasonal dependence of $\beta_s(t)$ accounts for the observed temperature dependence of *Bd* activity and growth [23, 24, 25] and possible variations in host behavior, which might explain the widely observed seasonal variation of *Bd* prevalence [26, 27, 13]. The exact form of $\beta_s(t)$ used in our simulations is given in section 1.4, and is parameterized by its time-average $\overline{\beta}_s$, its relative oscillation amplitude b and phase lag φ with respect to the host's breeding period.

In the deterministic limit (i.e. for large host populations), we obtain the dynamics

$$\begin{aligned}
\frac{d}{dt}P_\mathrm{A}(t,n) &= \left[\beta_\mathrm{A}(t)Z(t) + I_{\mathrm{A,u}}(n-1)\right]P_\mathrm{A}(t,n-1) \\
&+ I_{\mathrm{A,d}}(n+1)P_\mathrm{A}(t,n+1) \\
&- \left[\beta_\mathrm{A}(t)Z(t) + I_{\mathrm{A,u}}(n) + I_{\mathrm{A,d}}(n)\right]P_\mathrm{A}(t,n) \\
&- \left[\mu_\mathrm{A}(\mathbf{N}(t)) + g_\mathrm{A}(n)\right]P_\mathrm{A}(t,n) \\
&+ \frac{\delta_{n,0}}{\tau_\mathrm{m}}\sum_{n'=0}^{\infty}\sigma_\mathrm{m}(n')P_\mathrm{T}(t,n')
\end{aligned} \tag{1}$$

for adults and

$$\begin{aligned}
\frac{d}{dt}P_\mathrm{T}(t,n) &= \left[\beta_\mathrm{T}(t)Z(t) + I_{\mathrm{T,u}}(n-1)\right]P_\mathrm{T}(t,n-1) \\
&+ I_{\mathrm{T,d}}(n+1)P_\mathrm{T}(t,n+1) \\
&- \left[\beta_\mathrm{T}(t)Z(t) + I_{\mathrm{T,u}}(n) + I_{\mathrm{T,d}}(n)\right]P_\mathrm{T}(t,n) \\
&- \left[\mu_\mathrm{T}(\mathbf{N}(t)) + g_\mathrm{T}(n) + \frac{1}{\tau_\mathrm{m}}\right]P_\mathrm{T}(t,n) \\
&+ \delta_{n,0}r_\mathrm{br}(t)\sum_{n'=0}^{\infty}\sigma_\mathrm{br}(n')P_\mathrm{A}(t,n'),
\end{aligned} \tag{2}$$

for tadpoles. We assume the zoospore pool $Z(t)$ to be subject to (i) a free zoospore loss rate μ_Z, (ii) a zoospore influx at a rate $\sum_s \eta_s \sum_n P_s(t,n)n = \sum_s \eta_s N_s S_s$ from infected hosts and (iii) a constant supply from a possible environmental reservoir. The second term expresses the idea that the infectivity of a host increases with its fungal load. The parameter η_s corresponds to the average zoospore release rate per zoospore present on the skin of a host at life stage s [25]. This suggests the dynamics

$$\frac{dZ}{dt} = \sum_{s\in\{\mathrm{A,T}\}}\eta_s N_s(t)S_s(t) - \mu_\mathrm{Z}\cdot\left[Z(t) - Z_o\right]. \tag{3}$$

1.4 Used functional responses

Here, we give the exact functional responses $\sigma_\mathrm{br}(n)$, $\sigma_\mathrm{m}(n)$, $g_s(n)$, $I_{s,\mathrm{u}}(n)$, $I_{s,\mathrm{d}}(n)$, the breeding function $r_\mathrm{br}(t)$ and the transmission rates $\beta_s(t)$, used in our numerical simulations.

For the breeding function r_br, introduced in section 1.1, we used the wrapped Cauchy distribution [28, §3.5.7]

$$r_\mathrm{br}(t) = \frac{r}{Y}\frac{\sinh\left(2\pi\frac{\gamma}{Y}\right)}{\cosh\left(2\pi\frac{\gamma}{Y}\right) - \cos\left(2\pi\frac{t}{Y}\right)}, \tag{4}$$

centered at $t = 0$. Here, $\gamma > 0$ is a suitable shape parameter determined by the FWHM τ_br, defined such that $r_\mathrm{br}(\tau_\mathrm{br}/2) = (\max r_\mathrm{br} + \min r_\mathrm{br})/2$. For $\tau_\mathrm{br} \to Y^-/2$,

$\gamma \to \infty$ and $r_{\rm br}$ becomes constant r/Y. See fig. 1(a) for an illustration of $r_{\rm br}(t)$.

For the breeding factor $\sigma_{\rm br}(n)$ and the probability $\sigma_{\rm m}(n)$, introduced in section 1.1, we used

$$\sigma_{\rm br}(n) = \frac{1}{1+n/\mathcal{T}_{\rm br}}, \quad \sigma_{\rm m}(n) = \frac{1}{1+n/\mathcal{T}_{\rm m}}$$

which describe the simplest forms decaying to zero as n increases. Choosing $\mathcal{T}_{\rm br} = \infty$ sets $\sigma_{\rm br}(n) = 1$ for all n, and similarly for $\sigma_{\rm m}(n)$.

We assume that healthy adults and tadpoles suffer from (i) density independent, so called *base mortalities*, due to fatal random events, such as disturbances and predation and (ii) density dependent mortalities, e.g. due to intraspecific competition. Competition is assumed to only take place within the same life stage and to impose a constant stress on individuals. On the other hand, we assume that fatal events occur at a Poissonian rate. In the limit of very weak (i.e. affecting few individuals) but highly frequent fatal events, this corresponds to constant base mortality rates $\mu_s(0)$. Density dependence is reflected in a linear additive term, i.e.

$$\mu_s(\mathbf{N}) = \mu_s(0) + c_s N_s(t), \tag{5}$$

where $c_s > 0$ is a constant, in correspondence with the widely used logistic growth model [29].

For the *Bd* -induced mortality $g_s(n)$, introduced in section 1.2, we considered the form

$$g_s(n) = \frac{(\mathcal{F}_s - \mathcal{T}_s)\ln 2}{Y\mathcal{T}_s} \cdot \frac{n}{\mathcal{F}_s - n}, \tag{6}$$

which is one of the simplest function growing with the DOI and becoming infinite at a certain lethal DOI $\mathcal{F}_s$. The parameter $\mathcal{T}_s$ is such that $e^{-Y g_s(\mathcal{T}_s)} = 1/2$.

We assume that the within-host growth dynamics of *Bd* are determined by (i) an intrinsic zoospore death rate $\mu_{{\rm S},s}$, (ii) the infection of nearby tissue at a rate asymptotically growing with the square root of the DOI and (iii) the possible clearance of infection by the host's immune system at a rate asymptotically growing with the square root of the DOI. The second assumption is based on the simplifying view of a localized, monocentric, colonial growth of *Bd* on the host's skin [23, 19], at a rate proportional to the colony's outer perimeter. The third assumption is based on the related view that the host's innate immune response is mainly active on the perimeter of the localized infection. For simplicity, we only consider the net action of last two effects. This suggests that $I_{s,{\rm u}}(n) \sim \max(0,\alpha_s)\sqrt{n}$ as $n \to \infty$ and $I_{s,{\rm d}}(n) \sim \mu_{{\rm S},s} n - \min(0,\alpha_s)\sqrt{n}$ as $n \to 0$ for suitable constants $\mu_{{\rm S},s} > 0$, $\alpha_s \in \mathbb{R}$. We therefore postulate $I_{s,{\rm u}}(n) = \max(0,\alpha_s)\left[\sqrt{n+1}-1\right]$ and $I_{s,{\rm d}}(n) = \mu_{{\rm S},s} n - \min(0,\alpha_s)\left[\sqrt{n+1}-1\right]$. The somewhat special form for $I_{s,{\rm u}}$ and $I_{s,{\rm d}}$ ensures that $I_{s,{\rm u}}(0) = I_{s,{\rm d}}(0) = 0$ and that $I'_{s,{\rm u}}(0)$, $I'_{s,{\rm d}}(0)$ exist. In view of the early invasion analysis presented in section 2.3, we would like to parameterize the within-host dynamics with the zoospore mortality $\mu_{{\rm S},s}$ and the early growth rate $\lambda_s := I'_s(0)$ (which can be negative or positive), where $I_s := I_{s,{\rm u}} - I_{s,{\rm d}}$. We find that $\alpha_s = 2(\mu_s + \lambda_s)$, so that

$$\begin{aligned} I_{s,{\rm u}}(n) &= 2\max(0,\mu_{{\rm S},s}+\lambda_s)\left[\sqrt{n+1}-1\right], \\ I_{s,{\rm d}}(n) &= \mu_{{\rm S},s} n - 2\min(0,\mu_{{\rm S},s}+\lambda_s)\left[\sqrt{n+1}-1\right]. \end{aligned} \tag{7}$$

See fig. 1(b) for an illustration of the resulting expected DOI growth speed $I_s(n)$. Note that whenever $\lambda_s > 0$, there exists a unique DOI $K_{{\rm S},s} = 4\lambda_s(\lambda_s+\mu_s)/\mu_s^2 > 0$ with $I_s(K_{{\rm S},s}) = 0$. This *within-host capacity* $K_{{\rm S},s}$ gives a hypothetical slowly-changing transient DOI that the host will suffer from in the absence of secondary infections, before it either clears the infection or dies. If $K_{{\rm S},s} \geq \mathcal{F}_s$, infections self-perpetuate to ever increasing degrees and eventually lead to the host's death. Whenever $\lambda_s < 0$, $I_s(n) < 0$ for all n and self-reinfections can not compensate for the loss of zoospores.

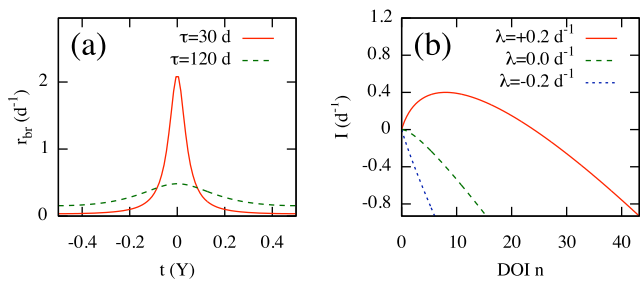

Figure 1: Illustration of the functional responses used in the simulations. (a) Breeding function $r_{\rm br}(t)$, as defined in (4), for $r = 100$ and varying FWHM $\tau_{\rm br}$. (b) Expected DOI growth speed $I(n) = I_{\rm u}(n) - I_{\rm d}(n)$ (life stage index s omitted), for $\mu_{\rm S} = 0.1$ and varying early growth rates λ.

For the transmission rates $\beta_s(t)$, introduced in section 1.3, we chose the widely adopted form [30]

$$\beta_s(t) = \overline{\beta}_s \cdot \left[1 + b \cdot \cos\left[2\pi\left(t-\varphi\right)/Y\right]\right].$$

Here, $b \in [0,1]$ is the relative amplitude of variation and $\varphi \in [0,1)$ is the phase-lag of the transmission rate's maximum with respect to the host's breeding period. Both b and φ are assumed equal for all life stages.

1.5 Host carrying capacities

Here, we comment on the host carrying capacities introduced in section 1.2. Defining carrying capacities in a non-autonomous model as the one use here, and relating them to the model parameters, is a non-trivial task, even

in the absence of disease. We therefore concentrate on the case of a time-independent breeding function $r_{\rm br} = r/Y$, where r is the yearly host fecundity introduced in section 1.1. In this case we obtain the simplified dynamics

$$\begin{aligned}\dot{N}_{\rm A} &= \frac{\sigma_{\rm m}(0)}{\tau_{\rm m}} N_{\rm T} - \left[\mu_{\rm A}(0) + c_{\rm A} N_{\rm A}\right] N_{\rm A},\\ \dot{N}_{\rm T} &= \frac{r}{Y}\sigma_{\rm br}(0) N_{\rm A} - \left[\frac{1}{\tau_{\rm m}} + \mu_{\rm T}(0) + c_{\rm T} N_{\rm T}\right] N_{\rm T}.\end{aligned} \tag{8}$$

The system (8) admits the non-trivial equilibrium $(N_{\rm A}, N_{\rm T}) = (K_{\rm A}, K_{\rm T})$ if and only if

$$\begin{aligned}c_{\rm A} &= \frac{1}{K_{\rm A}}\left[\frac{\sigma_{\rm m}(0)}{\tau_{\rm m}}\frac{K_{\rm T}}{K_{\rm A}} - \mu_{\rm A}(0)\right],\\ c_{\rm T} &= \frac{1}{K_{\rm T}}\left[\frac{r}{Y}\sigma_{\rm br}(0)\frac{K_{\rm A}}{K_{\rm T}} - \frac{1}{\tau_{\rm m}} - \mu_{\rm T}(0)\right],\end{aligned} \tag{9}$$

and provided the resulting competition coefficients $c_{\rm A}$, $c_{\rm T}$ turn out to be positive. A straightforward linear stability analysis of (8) shows that, if existing, the equilibrium $(K_{\rm A}, K_{\rm T})$ is in fact locally asymptotically stable.

For non-constant breeding functions $r_{\rm br}$ (but unchanged r), this equilibrium vanishes and the carrying capacities $K_{\rm A}, K_{\rm T}$ corresponding to the coefficients $c_{\rm A}, c_{\rm T}$ should be seen as an approximation of the *average* population sizes throughout the year. Simulations show that this interpretation is sufficiently accurate, at least for the considered breeding functions. We use $K_{\rm A}$, $K_{\rm T}$ as free parameters, replacing $c_{\rm A}$ and $c_{\rm T}$ via (9), when presenting our simulation results.

2 The mean field model

Here, we generalize the one-species, two-life-stages model introduced in section 1, to a community of multiple host species with multiple life stages. The index s thus runs through all species and life stages, referred to as *types* (k in total). In this context, $\mathbf{N} := (N_1, .., N_k)$ and $\mathbf{S} := (S_1, .., S_k)$. We derive a mean field approximation for the dynamics of the population sizes $\mathbf{N}$ and the mean DOIs $\mathbf{S}$. In section 2.2 we show the relationship of this model to standard SIR models of direct-contact density-dependent disease transmission. Furthermore, using the mean field approximation, in section 2.3 we investigate the early invasion dynamics of *Bd*. In section 2.4, we derive a host-demographic condition for a long-term endemic state of the fungus.

2.1 Derivation

Our starting point is a generalization of (1) and (2) to multiple species with multiple life stages and arbitrary recruitment fluxes. Hence, the index s now runs through all life stages of all species. We assume that at time t, individuals of type s within a community of population sizes $\mathbf{N}$ and with a DOI n, are lost at a rate $M_s(t, \mathbf{N}, n)$. We assume that at any time t, individual hosts of type s' and DOI n, induce the recruitment of hosts of type $s \neq s'$ at a rate proportional to their abundance $P_{s'}(t, n)$ and a *breeding function* $R_{s's}(t, n)$, similar to the breeding function introduced in section 1.1. For example, for the model presented in section 1, $R_{\rm T,A}(t, n) = \sigma_{\rm m}(n)/\tau_{\rm m}$ and $R_{\rm A,T}(t, n) = \sigma_{\rm br}(n) r_{\rm br}(t)$. The functional responses $I_{s,\rm u}$, $I_{s,\rm d}$, the parameters η_s, $\mu_{\rm Z}$ and transmission rates $\beta_s(t)$, introduced in section 1.3, maintain their original meaning. The zoospore mortality $\mu_{\rm Z}$ is now allowed to be time-dependent, while we omit any possible reservoir Z_o, so that

$$\frac{dZ}{dt} = \sum_{s=1}^{k} \eta_s N_s(t) S_s(t) - \mu_{\rm Z}(t) \cdot Z. \tag{10}$$

We assume that all newly recruited individuals are healthy. More precisely, we consider the dynamics

$$\begin{aligned}\frac{d}{dt}P_s(t,n) = {} & [\beta_s(t)Z(t) + I_{s,\rm u}(n-1)] \cdot P_s(t, n-1)\\ & + I_{s,\rm d}(n+1) \cdot P_s(t, n+1)\\ & - [\beta_s(t)Z(t) + I_{s,\rm u}(n) + I_{s,\rm d}(n)] \cdot P_s(t,n)\\ & - M_s(t, \mathbf{N}, n) \cdot P_s(t,n)\\ & + \delta_{n,0} \sum_{s' \neq s} \sum_{m=0}^{\infty} R_{s's}(t,m) P_{s'}(t,m).\end{aligned} \tag{11}$$

From (11) one quickly finds

$$\begin{aligned}\frac{d}{dt}N_s(t) &= \left[\widehat{R}_s(t) - \widehat{M}_s(t, \mathbf{N})\right] \cdot N_s(t),\\ \frac{d}{dt}S_s(t) &= \beta_s(t)Z(t) + \widehat{I}_{s,\rm u}(t) - \widehat{I}_{s,\rm d}(t)\\ &\quad - S_s(t) \cdot \widehat{R}_s(t)\\ &\quad - \widehat{\widehat{M}}_s(t, \mathbf{N}) + S_s(t) \cdot \widehat{M}_s(t, \mathbf{N}),\end{aligned} \tag{12}$$

where we temporarily defined the *mean field variables*

$$\begin{aligned}\widehat{R}_s(t) &:= \frac{1}{N_s(t)} \sum_{s' \neq s} \sum_{n=0}^{\infty} R_{s's}(t,n) P_{s'}(t,n),\\ \widehat{M}_s(t, \mathbf{N}) &:= \frac{1}{N_s(t)} \sum_{n=0}^{\infty} P_s(t,n) M_s(t, \mathbf{N}, n),\\ \widehat{\widehat{M}}_s(t, \mathbf{N}) &:= \frac{1}{N_s(t)} \sum_{n=0}^{\infty} P_s(t,n) M_s(t, \mathbf{N}, n) n,\\ \widehat{I}_{s,\rm u}(t) &:= \frac{1}{N_s(t)} \sum_{n=0}^{\infty} P_s(t,n) I_{s,\rm u}(n),\\ \widehat{I}_{s,\rm d}(t) &:= \frac{1}{N_s(t)} \sum_{n=0}^{\infty} P_s(t,n) I_{s,\rm d}(n).\end{aligned}$$

We approximate

$$R_{s's}(t,n) \approx R_{s's}(t,S_s) + R'_{s's}(t,S_s)\cdot(n-S_s),$$

and similarly for $M_s(t,\mathbf{N},n)$, $I_{s,\mathrm{u}}(n)$, $I_{s,\mathrm{d}}(n)$, where the prime $'$ refers to the derivative with respect to the DOI n. From (12), we finally obtain

$$\frac{dN_s}{dt} \approx [R_s(t,\mathbf{N},\mathbf{S}) - M_s(t,\mathbf{N},S_s)]\cdot N_s, \tag{13}$$

and

$$\begin{aligned}\frac{dS_s}{dt} \approx& \beta_s(t)\cdot Z + I_s(S_s)\\ &- S_s\cdot R_s(t,\mathbf{N},\mathbf{S}) - M'_s(t,\mathbf{N},S_s)\cdot V_s(t),\end{aligned} \tag{14}$$

where $I_s := I_{s,\mathrm{u}} - I_{s,\mathrm{d}}$. Here,

$$V_s(t) := \frac{1}{N_s(t)}\sum_{n=0}^{\infty}(n-S_s(t))^2 P_s(t,n)$$

is the DOI variance across the population and

$$R_s(t,\mathbf{N},\mathbf{S}) := \frac{1}{N_s(t)}\sum_{s'\neq s} R_{s's}(t,S_{s'})N_{s'}(t)$$

is an approximation for the per-capita recruitment rate of type s, depending on the community population sizes $\mathbf{N}$ and the average DOIs $\mathbf{S}$. For example, for the single-species model described in section 1,

$$\begin{aligned}R_{\mathrm{A}}(t,\mathbf{N},\mathbf{S}) &= \frac{N_{\mathrm{T}}}{N_{\mathrm{A}}}\frac{\sigma_{\mathrm{m}}(S_{\mathrm{T}})}{\tau_{\mathrm{m}}},\\ R_{\mathrm{T}}(t,\mathbf{N},\mathbf{S}) &= \frac{N_{\mathrm{A}}}{N_{\mathrm{T}}}\sigma_{\mathrm{br}}(S_{\mathrm{A}})r_{\mathrm{br}}(t).\end{aligned}$$

The approximations (13) and (14) become exact if $R_{s's}(t,n)$, $M_s(t,\mathbf{N},n)$, $I_{s,\mathrm{u}}(n)$ and $I_{s,\mathrm{d}}(n)$ are affine functions of n, or if the DOI distribution is very narrow. The latter case is unlikely, as macroparasite loads are typically overdispersed [31]. A result similar to (14) has been found for macroparasite dynamics by May *et al.* [32, eq. (19)–(21)] (although May *et al.* considered the total number of parasites, rather than the average parasite load per host). One difference of our model is the absence of a saturation of the force of infections for large host numbers, which would correspond to a zoospore depletion term $-\sum_s \beta_s N_s Z$ in (10). For related models, we refer to the review by Roberts *et al.* [33].

We note that the equation system (10), (13), (14) can not be readily integrated, since $V_s(t)$ still remains an unknown, time-dependent variable. However, this mean field approximation gives valuable insight into the epizootic dynamics of *Bd*, as every term in (14) allows for a special interpretation. The first term corresponds to an increase of infection load due to continuous exposure of individuals to the zoospore pool. The second term expresses the expected within-host disease dynamics. The third term corresponds to the reduction of the average DOI, resulting from a continuous recruitment of healthy individuals. The last term can be interpreted as follows: As the DOI variance increases across the population, *Bd* -induced mortality strongly differentiates between severely and mildly infected individuals. This differential survivorship tends to decrease the average DOI.

2.2 Relation to density-dependent transmission models

Here we show how the disease dynamics postulated in section 1.3 and generalized in section 2.1 to k host types, formally relate to standard SIR models of direct-contact density-dependent disease transmission. We let $Z_o = 0$. For simplicity, let $\eta_s = \eta$ be the same for all host types s. Assuming the characteristic time scales of the zoospore pool to be short compared to the epizootic dynamics, $Z(t)$ is approximately given by $(\eta/\mu_{\mathrm{Z}}(t))\cdot\sum_s N_s(t)S_s(t)$, from (10) [33, §6]. Let $U(t) := \sum_s P_s(t,0)$ denote the number of uninfected (*susceptible*) hosts, $V := \sum_s(N_s - U_s)$ the number of infected hosts, $\widetilde{S} := \sum_s N_s S_s/V$ the average DOI of infected hosts and

$$\widetilde{\beta}(t) := \frac{1}{U(t)}\sum_s \beta_s(t)P_s(t,0)$$

the average transmission rate for uninfected hosts. The rate at which uninfected hosts of type s become infected, is given by $\beta_s(t)\eta V\widetilde{S}P_s(t,0)/\mu_{\mathrm{Z}}$, from (11). Summing over all types, we obtain

$$\frac{dV(t)}{dt} = V(t)U(t)\cdot\frac{\eta\widetilde{\beta}(t)}{\mu_{\mathrm{Z}}(t)}\widetilde{S}(t) - \ldots, \tag{15}$$

where the "…" represent host deaths and clearance of infections (*recovery*). (15) gives the density-dependent rate of new infections, with the (non-constant) *transmission coefficient* $\eta\widetilde{\beta}/\mu_{\mathrm{Z}}$ modulated by the *virulence* $\widetilde{S}$.

2.3 Early invasion dynamics

Here, we elaborate on the early invasion dynamics presented in section 3.1 of the main article. Our starting point is the mean field approximation derived in section 2.1, summarized by (10), (13) and (14). We assume $M'_s(t,\mathbf{N},0) = 0$, i.e. differential mortality only appears at high DOIs.

Suppose the *Bd* -free community has settled on a periodic orbit, $\mathbf{N}(t)$, of period T (e.g. $T = Y$ for an annual cycle). Upon exposure, the early exponential growth rate of *Bd*, ρ, is given by the maximal Lyapunov exponent [34] of the disease-free periodic orbit with respect to $(\mathbf{S}, Z)$,

i.e.

$$\rho = \sup_{\mathbf{y}} \lim_{t\to\infty} \frac{1}{t} \ln \left\| \Pi_{(\mathbf{S},Z)} \nabla_{\mathbf{x}} \phi(t, t_o, \mathbf{x}) \big|_{\mathbf{x}=\mathbf{x}_o} \mathbf{y} \right\|.$$

Here, $\mathbf{x} = (\mathbf{N}, \mathbf{S}, Z)$, $\mathbf{x}_o = (\mathbf{N}(t_o), 0, 0)$ is some point on the orbit at time t_o, $\phi(t, t_o, \mathbf{x})$ is the flow of the non-autonomous dynamical system (10), (13) and (14) [35, §3.4] and $\Pi_{(\mathbf{S},Z)}$ is the orthogonal projection on the components $(\mathbf{S}, Z)$. Let $J \in \mathbb{R}^{(2k+1)\times(2k+1)}$ denote the Jacobian associated with the dynamics. Note that J generally depends on time, $\mathbf{N}$, $\mathbf{S}$ and Z. One finds

$$J\big|_{(\mathbf{S},Z)=0} = \begin{pmatrix} A_1(t,\mathbf{N}) & A_2(t,\mathbf{N}) \\ 0 & J_o(t,\mathbf{N}) \end{pmatrix}, \tag{16}$$

where $A_1(t,\mathbf{N}) \in \mathbb{R}^{k\times k}$, $A_2(t,\mathbf{N}) \in \mathbb{R}^{k\times(k+1)}$ are matrices that depend on time and $\mathbf{N}$, and

$$J_o(t,\mathbf{N}) := \begin{pmatrix} \lambda_1 - R_1(t,\mathbf{N},0) & \dots & 0 & \beta_1(t) \\ \vdots & \ddots & \vdots & \vdots \\ 0 & \dots & \lambda_k - R_k(t,\mathbf{N},0) & \beta_k(t) \\ \eta_1 N_1 & \dots & \eta_k N_k & -\mu_{\mathrm{Z}}(t) \end{pmatrix}.$$

Here, $\lambda_s := I_s'(0)$ is the early, expected, within-host *Bd* growth rate. The sub-Jacobian J_o determines the linear dynamics of *Bd* near the disease-free periodic orbit of the community. The special structure of (16) implies that ρ is given by the spectral bound [36, 37] of the averaged matrix

$$\overline{J}_o := \frac{1}{T}\int_0^T J_o(t,\mathbf{N}(t))\, dt.$$

Denoting

$$\begin{aligned} \overline{N}_s &:= \frac{1}{T}\int_0^T N_s(t)\, dt, \\ \overline{\mu}_{\mathrm{Z}} &:= \frac{1}{T}\int_0^T \mu_{\mathrm{Z}}(t)\, dt, \\ \overline{\beta}_s &:= \frac{1}{T}\int_0^T \beta_s(t)\, dt, \\ \overline{R}_s &:= \frac{1}{T}\int_0^T R_s(t,\mathbf{N}(t),0)\, dt, \end{aligned} \tag{17}$$

allows us to write $\overline{J}_o$ as

$$\overline{J}_o = \begin{pmatrix} \lambda_1 - \overline{R}_1 & \dots & 0 & \overline{\beta}_1 \\ \vdots & \ddots & \vdots & \vdots \\ 0 & \dots & \lambda_k - \overline{R}_k & \overline{\beta}_k \\ \eta_1 \overline{N}_1 & \dots & \eta_k \overline{N}_k & -\overline{\mu}_{\mathrm{Z}} \end{pmatrix}. \tag{18}$$

If $\lambda_s - \overline{R}_s \geq 0$ for any type s, (18) has positive spectral bound, as can be seen using Grönwall's inequality [38]. We therefore concentrate on the case where $\lambda_s - \overline{R}_s < 0$ for all types s.

Notice the formal similarity of (18) to the transmission matrix of standard, class-structured, epidemic SI models [39], with S_s corresponding to the *number of infected individuals* of class s. We decompose J into a contact matrix

$$C := \begin{pmatrix} 0 & \dots & 0 & \overline{\beta}_1 \\ \vdots & & \vdots & \vdots \\ 0 & \dots & 0 & \overline{\beta}_k \\ \eta_1 \overline{N}_1 & \dots & \eta_k \overline{N}_k & 0 \end{pmatrix},$$

and a mortality matrix

$$G := \begin{pmatrix} \lambda_1 - \overline{R}_1 & \dots & 0 & 0 \\ \vdots & & \vdots & \vdots \\ 0 & \dots & \lambda_k - \overline{R}_k & 0 \\ 0 & \dots & 0 & -\overline{\mu}_{\mathrm{Z}} \end{pmatrix},$$

such that $J = C + G$. The basic reproduction quotient Q_o of *Bd* is then given by the spectral radius of the transmission matrix $K = -CG^{-1}$ [40, 41]. The latter is easily calculated and one obtains

$$Q_o = \frac{1}{\overline{\mu}_{\mathrm{Z}}} \sum_{s=1}^{k} \frac{\eta_s \overline{\beta}_s \overline{N}_s}{\overline{R}_s - \lambda_s}. \tag{19}$$

Notice that Q_o can also be derived heuristically in a simpler way: Since $1/\overline{\mu}_{\mathrm{Z}}$ is the expected life time of a single free zoospore, $\overline{\beta}_s N_s/\overline{\mu}_{\mathrm{Z}}$ gives the expected number of hosts of type s infected by that zoospore. The average turnover rate of zoospores on hosts of type s is $\overline{R}_s - \lambda_s$. Hence, $\eta_s/(\overline{R}_s - \lambda_s)$ gives an estimate for the number of new zoospores released into the water, per zoospore located on hosts of type s. Thus, the expected number of zoospores released into the water, originating from a single free zoospore, is given by (19). This recovers the epidemiological interpretation of Q_o, which might have been lost in the mathematical analogy made to SI models.

Alternatively, one might attempt to calculate the early *Bd* growth rate ρ directly from $\overline{J}_o$. We shall derive a two-term asymptotic approximation of ρ in the limit $\gamma_s \approx 0$ [42], where we abbreviate $\gamma_s := \lambda_s - \overline{R}_s$. We formally introduce the scaling parameter $\varepsilon \ll 1$ and let $\gamma_s = \varepsilon\gamma_s^o$, where $\gamma_s^o \in \mathcal{O}(1)$. The eigenvalue equation for $\overline{J}_o$ in ρ can be computed by applying Laplace's expansion rule to the first column. One obtains

$$\begin{aligned} 0 =& (\rho + \overline{\mu}_{\mathrm{Z}}) \prod_{s=1}^{k} (\rho - \gamma_s) \\ &- \sum_{s'=1}^{k} \eta_{s'} \overline{\beta}_{s'} \overline{N}_{s'} \prod_{s\neq s'} (\rho - \gamma_s). \end{aligned} \tag{20}$$

We expand $\rho = \rho_o + \varepsilon\rho_1 + \mathcal{O}(\varepsilon^2)$. Note that for $\varepsilon = 0$, $\rho = 0$ is a root of (20) of multiplicity $(k-1)$. The remaining two eigenvalues are real, one being negative and one positive. We are interested in the perturbation of the principal eigenvalue as ε is increased, so that $\rho_o > 0$. From (20) we obtain to leading order

$$(\rho_o + \overline{\mu}_{\mathrm{Z}})\rho_o = \sum_{s=1}^{k} \eta_s \overline{\beta}_s \overline{N}_s. \tag{21}$$

To second order, we find

$$\rho_1 = \left[\rho_o^2 + \sum_{s=1}^{k} \eta_s \overline{\beta}_s \overline{N}_s\right]^{-1} \sum_{s=1}^{k} \eta_s \overline{\beta}_s \overline{N}_s \gamma_s^o. \tag{22}$$

Combining (21) and (22), finally yields the approximation

$$\rho \approx \rho_o + \frac{\sum_s \eta_s \overline{\beta}_s (\lambda_s - \overline{R}_s)\overline{N}_s}{\rho_o^2 + \sum_s \eta_s \overline{\beta}_s \overline{N}_s}. \tag{23}$$

Fitting (23) to epizootic data, might give estimates of *Bd* transmission rates in natural habitats, as demonstrated in section 4.2.

We mention that certain species have been found to clear infections within as little as a few weeks [43, 8], while *Bd* in culture grows at similar time scales [25]. Epizootic outbreaks have also been found to occur at comparable time scales (e.g. $\rho \approx 0.15$ d^{-1} [11]), though turnover rates are usually one order of magnitude lower [1]. These cases seemingly violate the assumption $\left|\lambda_s - \overline{R}_s\right| \ll \rho$. Nevertheless, (23) illustrates the positive feedback loops operating between within-host disease dynamics and the zoospore pool Z.

2.4 Endemic states

Here we derive a host-demographic condition for the long-term persistence of *Bd* in an endemic state, in the absence of an environmental reservoir ($Z_o = 0$). Our starting point is the mean field approximation derived in section 2.1. We assume the amphibian community and the fungus to be on a stable, enzootic periodic orbit $(\mathbf{N}(t), \mathbf{S}(t), Z(t))$ of period T. We assume that the average DOI of the community is so low that (i) the within-host dynamics of *Bd* are described by the linearization $I_s(S_s) \approx \lambda_s S_s$, with λ_s as introduced in section 2.3, and (ii) the differential mortality of hosts due to *Bd*, i.e. the last term in (14), can be neglected in the dynamics of *Bd*. Then the dynamics (10), (13) and (14) take the form

$$\begin{pmatrix} \dot{\mathbf{S}}(t) \\ \dot{Z}(t) \end{pmatrix} = J_o(t, \mathbf{N}(t), \mathbf{S}(t)) \cdot \begin{pmatrix} \mathbf{S}(t) \\ Z(t) \end{pmatrix},$$

where

$$J_o(t, \mathbf{N}, \mathbf{S}) := \begin{pmatrix} \lambda_1 - R_1(t, \mathbf{N}, \mathbf{S}) & \dots & 0 & \beta_1(t) \\ \vdots & \ddots & \vdots & \vdots \\ 0 & \dots & \lambda_k - R_k(t, \mathbf{N}, \mathbf{S}) & \beta_k(t) \\ \eta_1 N_1 & \dots & \eta_k N_k & -\mu_{\mathrm{Z}}(t) \end{pmatrix}.$$

Periodicity of the orbit requires that

$$\exp\left[T\overline{J}_o\right] \cdot \begin{pmatrix} \mathbf{S}(0) \\ Z(0) \end{pmatrix} = \begin{pmatrix} \mathbf{S}(0) \\ Z(0) \end{pmatrix},$$

where

$$\overline{J}_o := \frac{1}{T}\int_0^T J_o(t, \mathbf{N}(t), \mathbf{S}(t))\, dt$$

is the average Jacobian along the orbit. This means that $\exp\left[T\overline{J}_o\right]$ has the eigenvalue 1, which is equivalent to $\overline{J}_o$ having zero determinant. Using Laplace's expansion rule, this translates to the condition

$$\begin{aligned} 0 =& \overline{\mu}_{\mathrm{Z}} \prod_{s=1}^{k} (\lambda_s - \overline{R}_s) \\ &+ \sum_{s'=1}^{k} \eta_{s'} \overline{\beta}_{s'} \overline{N}_{s'} \prod_{s \neq s'} (\lambda_s - \overline{R}_s), \end{aligned} \tag{24}$$

where $\overline{N}_s$, $\overline{\beta}_s$ and $\overline{\mu}_{\mathrm{Z}}$ are defined as in (17) and

$$\overline{R}_s := \frac{1}{T}\int_0^T R_s(t, \mathbf{N}(t), \mathbf{S}(t))\, dt.$$

In the generic case, $\lambda_s \neq \overline{R}_s$, so that (24) finally translates to

$$\frac{1}{\overline{\mu}_{\mathrm{Z}}} \sum_{s=1}^{k} \frac{\eta_s \overline{\beta}_s \overline{N}_s}{\overline{R}_s - \lambda_s} \approx 1. \tag{25}$$

We note that the assumption of a periodic orbit is not crucial, and can easily be replaced by the assumption that *Bd* prevalence stays bounded for long times.

Also note that (25) is a condition for the long-term prevalence of the fungus, and not the host community. If the demographic variables $\overline{N}_s$ and $\overline{R}_s$ are available, (25) can be used to estimate some of the epizootic parameters. This is demonstrated in section 4.2. Moreover, comparing (25) to (19) demonstrates the following principle: While the initial invasion of the fungus requires a sufficiently large host population to establish itself, a long-term stabilization on an endemic state only occurs once the host population has sufficiently decreased.

3 Modelling delayed tadpole metamorphosis

In this section we describe a modification of the model introduced in section 1, to account for possible delays in the onset of metamorphosis. We recall that, as postulated in section 1.1, tadpoles were assumed to metamorphose at a Poissonian rate which is independent of their age, therefore exhibiting exponentially distributed life times of mean τ_{m}. As an alternative on the other side of the spectrum, we considered the case where tadpoles do not metamorphose at all for a fixed time τ_{m}, and then instantaneously attempt metamorphosis. This modification requires an age structured population model, which keeps track of the distribution of tadpole ages.

3.1 The mathematical model

Extending the terminology of the original model, we denote by $P_{\mathrm{T}}(t,\alpha,n)$ the density of tadpoles at age α, with DOI n. Note that then $P_{\mathrm{T}}(t,n)=\int_0^{\tau_{\mathrm{m}}} P_{\mathrm{T}}(t,\alpha,n)\,d\alpha$. We keep the assumption of age-independent adult fecundity, so we do not need to keep track of the age distribution of adults. Adapting the mechanisms and fluxes of the original model, leads to the following dynamics

$$\begin{aligned}
&\frac{d}{dt}P_{\mathrm{A}}(t,n)=\left[\beta_{\mathrm{A}}(t)Z(t)+I_{\mathrm{A,u}}(n-1)\right]P_{\mathrm{A}}(t,n-1)\\
&+I_{\mathrm{A,d}}(n+1)P_{\mathrm{A}}(t,n+1)\\
&-\left[\beta_{\mathrm{A}}(t)Z(t)+I_{\mathrm{A,u}}(n)+I_{\mathrm{A,d}}(n)\right]P_{\mathrm{A}}(t,n)\\
&-\left[\mu_{\mathrm{A}}(N_{\mathrm{A}}(t))+g_{\mathrm{A}}(n)\right]P_{\mathrm{A}}(t,n)\\
&+\delta_{n,0}\sum_{mn'0}^{\infty}\sigma_{\mathrm{m}}(n')P_{\mathrm{T}}(t,\tau_{\mathrm{m}},n')
\end{aligned}\tag{26}$$

for adults and

$$\begin{aligned}
&\partial_t P_{\mathrm{T}}(t,\alpha,n)\\
=&\left[\beta_{\mathrm{T}}(t)Z(t)+I_{\mathrm{T,u}}(n-1)\right]P_{\mathrm{T}}(t,\alpha,n-1)\\
&+I_{\mathrm{T,d}}(n+1)P_{\mathrm{T}}(t,\alpha,n+1)\\
&-\left[\beta_{\mathrm{T}}(t)Z(t)+I_{\mathrm{T,u}}(n)+I_{\mathrm{T,d}}(n)\right]P_{\mathrm{T}}(t,\alpha,n)\\
&-\left[\mu_{\mathrm{T}}(N_{\mathrm{T}}(t))+g_{\mathrm{T}}(n)\right]P_{\mathrm{T}}(t,\alpha,n)\\
&-\partial_\alpha P_{\mathrm{T}}(t,\alpha,n)
\end{aligned}\tag{27}$$

for tadpoles, with boundary condition

$$P_{\mathrm{T}}(t,0,n)=\delta_{n,0}r_{\mathrm{br}}(t)\sum_{n'=0}^{\infty}\sigma_{\mathrm{br}}(n')P_{\mathrm{A}}(t,n'). \tag{28}$$

The last line in (27) corresponds to the steady progression of individual age. The boundary condition (28) is necessary since (27) is now a partial differential equation, and corresponds to the influx of new, non-infected tadpoles of age 0. All other terms remain similar to the original model. The dynamics of the zoospore pool $Z(t)$, given by (3), also remain unchanged.

We mention that for the above model, a mean field approximation can be derived similarly to section 2 (equations (13) and (14)), although some additional terms appear due to potential differences of the DOI distribution among different age groups. If one assumes that in the early invasion phase the DOI distribution is uniform across various tadpole ages, then the basic reproduction quotient (19) can be derived in a similar way to section 2.3.

3.2 Numerical simulations

Using numerical simulations, we investigated the dynamics of the modified model introduced in section 3.1. We focused on the role of tadpoles as a potential reservoir for *Bd* or rescue buffer for the host population. Due to the explicit age structure, the numerical code differs significantly from the original one. Instead of directly integrating the master equations (26) and (27), we implemented a stochastic individual based model [44], that keeps track of the DOI and age of individual adults and frogs. Individual DOI transitions, deaths and the creation of tadpoles occur randomly at the rates given by the master equations (26) and (27). Tadpoles attempt metamorphosis as soon as they reach age τ_{m}. Metamorphosing tadpoles with DOI n' are moved to the adult pool with zero DOI at a probability $\sigma_{\mathrm{m}}(n')$, or are discarded otherwise. The zoospore pool dynamics (3) are integrated just as in the original model.

3.3 Results

For similar parameter values far from critical points, simulations showed a behaviour qualitatively similar to the original model. However, we observed that the parameter space for which the host population persists for longer times (even in the absence of disease), is smaller than for the original model. In particular, stable tadpole carrying capacities are higher in this model because of the delayed onset of metamorphosis. Furthermore, the prolonged tadpole stage exposes tadpoles to a higher cumulative risk of death, before they can contribute to the adult population. Therefore, host survivorships are generally required to be higher than in the original model.

We were particularly interested in investigated the role of tadpoles as potential reservoir for *Bd* or rescue buffer for an otherwise stressed host population. To that extent, we repeated the simulations of the original model, reported in section 3.4 of the main article (figures 2(a–d) and 3(a,b)). Our findings remain qualitatively valid for the case of delayed metamorphosis, when taking into account the general differences of the two models described in the previous paragraph. In particular, we find that if

the zoospore loss rate is high, then long living tadpoles that tolerate *Bd* tend to destabilise the epizootic and lead to strong occasional outbreaks, due to delays in the host-parasite population feedback loop (figures 2(a,b)). Both a shorter tadpole life stage or a susceptibility of tadpoles to *Bd* can stabilise the epizootic at a low *Bd* prevalence level (figures 2(c,d)). On the other hand, if *Bd* can persist for long times, either as free zoospores or within hosts, then a susceptibility of tadpoles can have opposite effects and in fact tends to increase the risk of extinction (figures 3(a,b)). This is again similar to our findings from the first model, and underlines the ambivalence of the role of tadpoles.

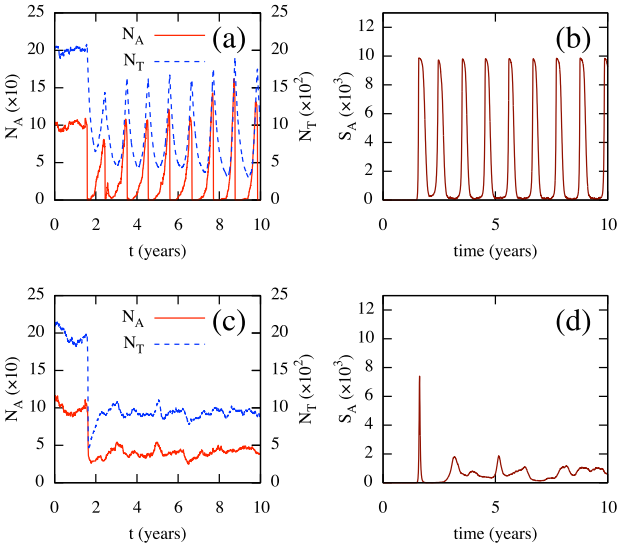

Figure 2: Simulations of the individual based model with delayed metamorphosis, described in section 3 (one per row). The host population is exposed to *Bd* during the 2nd year, resulting in an endemic state similar to figures 2(a–d) in the main article. Figures (a,c) show population sizes, figures (b,d) show the mean adult DOI. The breeding rate r_{br} and transmission rates $\overline{\beta}_{\mathrm{A}}$, $\overline{\beta}_{\mathrm{T}}$ are time-independent. (a,b): Tadpoles do not suffer from infection and have a long life time ($\tau_{\mathrm{m}} = Y$). The observed cycles are purely due to host-demographic delays involved in the response to the epizootic, as *Bd*-intrinsic time scales are very short ($\mu_{\mathrm{Z}} = 1\ \mathrm{d}^{-1}$, $\mu_{\mathrm{S,A}} = \mu_{\mathrm{S,T}} = 0.2\ \mathrm{d}^{-1}$). (c,d): Tadpoles strongly suffer from infection, but with otherwise identical parameters as in (a,b). Notice the absence of strong epizootic outbreaks compared to (a,b). Shorter tadpole life stages have similar stabilising effects. Model parameters given in table 1. Notice the similarity of these results to figures 2(a–d) in the main article.

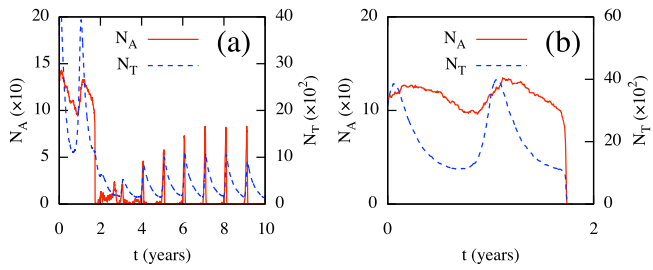

Figure 3: Two similar simulations of the individual based model with delayed metamorphosis, described in section 3. Graphs show adult and tadpole population sizes. Annual peaks coincide with breeding seasons. The host population is exposed to the fungus during the second year. (a): Tadpoles do not suffer from infection and enable host survival, albeit at a reduced population size. (b): Tadpoles suffer from infection, all other parameters are identical to (a). Upon exposure to the fungus, the population quickly goes extinct. Model parameters given in table 1. Compare these results to figures 3(a,b) in the main article.

4 Estimating epizootic parameters

4.1 Parameters of within-host disease dynamics

In the following, we illustrate how time series of the DOI of infected individuals, obtained for example experimentally [10, 12], might be used to estimate various parameters of the postulated within-host disease dynamics and associated mortalities. Our starting point are the transition rates $I_{s,\mathrm{u}}$ and $I_{s,\mathrm{d}}$ introduced in section 1.3 and the disease induced mortality rate g_s introduced in section 1.2. For simplicity, we omit the life stage index s. For high zoospore loads $x \gg 1$, the expected value of the birth-death process associated with the probability rates $I_{\mathrm{u}}, I_{\mathrm{d}}$ can be replaced by the trajectory described by the deterministic growth speed $dx/dt = I(x) = I_{\mathrm{u}}(x) - I_{\mathrm{d}}(x)$. If the observed temporal evolution of infections does not differ much between individuals (up to the point of death), and if infections are monotonic (either non-decreasing or non-increasing), the trajectory $x(t)$ can be fitted to the measured DOI time series to obtain estimates for the parameters defining I.

On the other hand, the stochasticity of possible infection loads, as well as the finite death rate induced by them, contribute to the temporal unpredictability of host death. The probability of an infected individual being alive at post-exposure time T, is given by

$$\sigma(T) = \exp\left[-\int_0^T \sum_n g(n)p(t,n)\ dt\right] \cdot \sigma_o(T), \qquad (29)$$

where $\sigma_o(T)$ is the (base) survivorship of uninfected controls at time T, and $p(t,n)$ is the probability of having DOI n at time t, conditional upon being alive. Estimating the distribution $p(t,n)$ and the survival curve $\sigma(T)$ experimentally, might give an approximation for the parameters determining the mortality $g(n)$. Suppose, for example, that $g(n)$ can be approximated by a mortality increasing linearly with the DOI, i.e., let $g(n) \approx g'(0) \cdot n$. Then (29) predicts

$$\sigma(T) \approx \exp\left[-g'(0) \cdot \int_0^T x(t)\ dt\right] \cdot \sigma_o(T), \qquad (30)$$

where $x(t)$ is the expected DOI at time t. Approximating $x(t)$ by the mean DOI measured on living individuals, provides a means for estimating $g'(0)$. We illustrate this procedure for the following simple case: Suppose that the sample-mean DOI can be approximated by the logistic growth model $dx/dt = \lambda x \cdot (1 - x/K)$ of a within-host zoospore population with carrying capacity K_S, early growth rate λ and initial size $x(0) = x_o$. Such an approximation might be suitable for DOI time series exhibiting initial exponential growth and a transient settlement on a constant value. Also assume a constant base mortality rate $\mu_o \geq 0$. Then (30) can be explicitly evaluated to give

$$\sigma(T) \approx \left[1 + \frac{x_o}{K_\mathrm{S}}\left(e^{\lambda T} - 1\right)\right]^{-\frac{K_\mathrm{S}}{\lambda} g'(0)} \cdot e^{-\mu_o T}. \qquad (31)$$

Fitting (31) to measured survival curves, can provide estimates for μ_o (if not known) and $g'(0)$. See fig. 4 for an example.

4.2 Transmission rates

Transmission modes and transmission rates are of central central importance to epizootic models [45], and various attempts have been made to measure them [46, 13]. We shall demonstrate how our analytical results given in sections 2.3 and 2.4 can be used to estimate *Bd* transmission rates, based on either the growth rate of an epizootic outbreak or the demographic variables of a population in an endemic state.

Fitting the predicted growth rate (23) to epizootic data might provide a more accurate estimate for the transmission rates. Ignoring any within-host dynamics, such as the host's immune response, (21) gives the early epizootic growth rate $\rho \approx \rho_o$. Assuming that the zoospore release rate η_s is similar for different host types s, $(\rho + \mu_\mathrm{Z})\rho \approx \eta\widetilde{\beta}\ \overline{N}$, where $\overline{N} := \sum_s \overline{N}_s$ and $\widetilde{\beta} := \sum_s \overline{\beta}_s \overline{N}_s / \overline{N}$ is the mean transmission rate. [11] provide temporal data of *Bd* invasion in several mountain yellow-legged frog populations. They report a rate of increase of $\rho \approx 0.15\ \mathrm{d}^{-1}$ for

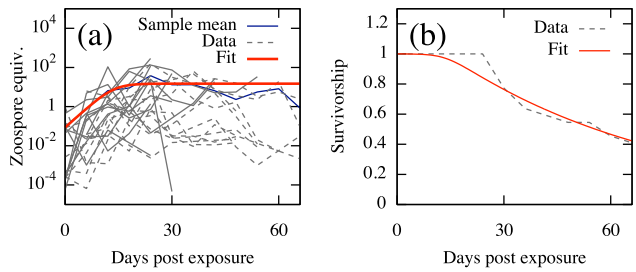

Figure 4: On estimating parameters of within-host *Bd* dynamics and mortalities, as described in section 4.1. (a) DOI time series of 22 experimentally infected *D. meridensis* frogs (Lampo, 2013, unpublished data), with fitted logistic growth curve. A least squares fit gives $\lambda = (0.38 \pm 0.60)\ \mathrm{d}^{-1}$, $K_\mathrm{S} = 14.9 \pm 3.6$ and $x_o = 0.086 \pm 0.687$. Adopting λ and K_S to the within-host model (7), gives a within-host loss rate $\mu_\mathrm{S} \approx 0.25\ \mathrm{d}^{-1}$, well within the range reported for *Bd* in culture [25]. (b) Survivorship over time for the same frogs, together with fitted curve (31). A least squares fit gives $g'(0) = 0.0011 \pm 0.0000007$ and $\mu_o = 0$. For $g(n)$ given by (7), with $\mathcal{F} \gg \mathcal{T}$, one obtains $\mathcal{T} \approx 1.73$.

the average DOI among eight similar populations. Pre-exposure population sizes were estimated between approximately 50 and 650 hosts (adults + subadults). Taking $\eta_s \approx 1.5$–$5.7\ \mathrm{d}^{-1}$ and $\mu_\mathrm{Z} \approx 0.02$–$1\ \mathrm{d}^{-1}$ (see section 5.1), estimates $\widetilde{\beta}$ between approximately $7 \times 10^{-6}\ \mathrm{d}^{-1}$ and $2 \times 10^{-3}\ \mathrm{d}^{-1}$. Since the actual population sizes (including tadpoles) are expected to have been much higher, we are most likely overestimating the actual transmission rate.

The equilibrium condition (25) presented in section 2.4 provides an alternative way of estimating transmission rates. Lampo *et al.* [1] estimated the population size (median of 93 adults) and recruitment rates (on average 165 frogs per year) for a *A. cruciger* population in Venezuela, coexisting with *Bd* at relatively low prevalence (9.6% detectable infected cases). Taking $\eta_\mathrm{A} \approx 1.5$–$5.7\ \mathrm{d}^{-1}$, $\mu_\mathrm{Z} \approx 0.02$–$1\ \mathrm{d}^{-1}$, while ignoring within-host dynamics ($\lambda_s \approx 0$) and only considering adults, estimates β_A between approximately $2 \times 10^{-7}\ \mathrm{d}^{-1}$ and $3 \times 10^{-5}\ \mathrm{d}^{-1}$.

5 Details of numerical methods

Here we comment on the numerical methods used to investigate the single species model presented in section 1 of this supplement and outlined in section 2.1 of the main article. In section 5.1 we justify the ranges considered for our model parameters, summarised in table 1 of the main article. Section 5.2 elaborates on the statistical methods we used to sample these ranges. Table 1 gives the values used in the various simulations presented in the main ar-

ticle. Section 5.3 elaborates on the stochastic version of our model.

We used an ad-hoc, explicit, second-order Runge-Kutta solver implemented in C++ [47]. The integration time step, dt, varied from 10^{-3} to 10^{-2} d, and was chosen such that any further reduction did not significantly change the simulation results. Simulations were typically run for 10 years, but complicated scenarios were investigated for up to 10^2 years. All simulations were started with a healthy host population near its carrying capacities K_A, K_T. In the middle of the second year, a single infected adult with DOI 10^3 was introduced into the population. Compared to the considered carrying capacities K_s, a single infected frog corresponds to the early onset of the epizootic, when *Bd* prevalence is still low.

The deterministic dynamics described in section 1 can never lead to the total extinction of hosts nor the total clearance of *Bd*, as is typical for continuous population dynamical models. In practice, a population can be considered extinct if its size falls below a certain threshold value. For amphibians, any such threshold size is at least two individuals, though Allee effects might push such a threshold further up. We considered the host population to be extinct as soon as the total number of tadpoles and adults fell below 2. We considered *Bd* to be cleared from the site, as soon as the total number of free and within-host zoospores fell below 10.

For optimization reasons, the range of possible DOIs, from 0 up to $\mathcal{F}_s$, was split into $m = 100$ *bins*. Thus, each DOI bin corresponded to $\mathcal{F}_s/m$ different degrees of infection. The Markovian transition rates given in (1) were rescaled accordingly by a factor $m/\mathcal{F}_s$. Further increasing the number of bins did not significantly affect the simulations.

5.1 Justification of parameter ranges

Here, we elaborate on our choice of parameters for our simulations, summarised in table 1 of the main article. The free zoospore death rate μ_Z has been estimated by Woodhams *et al.* [25] through laboratory experiments on *Bd* culture between 0.0648 d^{-1} (at 4.0°C) and 0.984 d^{-1} (at 28.0°C). Johnson *et al.* [48] find that *Bd* can remain infectious in lake water for up to 7 weeks ($\mu_\mathrm{Z} \approx 0.02\ \mathrm{d}^{-1}$). As a first guess, we set the lower bound of $\mu_{\mathrm{S},s}$ to the lower bound of μ_Z.

Furthermore, the model used by Woodhams *et al.* [25, equations (4) – (6)] predicts an asymptotic zoospore release rate $\eta \approx \lambda + \mu_\mathrm{Z} + m_\mathrm{Z}$, where λ is the intrinsic growth rate and m_Z the per capita zoospore encystment rate. Using their estimates for λ and m_Z (table 2 in original article), one obtains an estimate for η between 1.536 d^{-1} (at 10°C) and 5.714 d^{-1} (at 23°C).

Certain species have been found to clear their infection within as little as a few days [7, 8] or weeks [43]. This suggests a lower bound $\lambda_s \gtrsim -1\ \mathrm{d}^{-1}$ for the early *Bd* growth (or clearance) rates and an upper bound $\mu_{\mathrm{S},s} \lesssim 1\ \mathrm{d}^{-1}$ for the asymptotic on-host decay rates. Carey *et al.* [10] give the estimate $\lambda_\mathrm{A} \approx 0.68\ \mathrm{d}^{-1}$ for the growth rate of the fungus on boreal toads. As an upper bound for λ_s we used the optimal growth rates (approximately 1 d^{-1} at 23°C) reported by Woodhams *et al.* [25].

Throughout the article, fungal load and DOI refers to values reported from TaqMan real-time PCR assays with standardized swabbing [49]. The lethal DOI threshold generally depends on the considered species, life stage and the host's physical condition [50]. Epizootic observations by Vredenburg *et al.* [11] indicate an onset of mass mortality of *R. muscosa* and *R. sierrae*, at average loads of 10^4 to 10^5 zoospores per standardized swap. Similar findings from laboratory experiments on *L. booroolongensis* have been reported by Cashins *et al.* [12]. These values are expected to underestimate the true lethal fungal load, but they provide an estimate for the order of magnitude of $\mathcal{F}_\mathrm{A}$. Tadpole vulnerability to *Bd* is far from uniform across species, and some species seem to be unaffected by infection [2, 5]. Our choices of $\mathcal{F}_\mathrm{T} \sim \mathcal{F}_\mathrm{A}$ and $S_{\mathrm{T,max}}$, should therefore be treated with caution. The wide ranges considered for the host tolerances $\mathcal{T}_s$ and metamorphosing tolerance $\mathcal{T}_\mathrm{m}$, are dictated by their great uncertainty and variability across different species. For $\mathcal{T}_\mathrm{m} = \infty$, *Bd* has no effect on metamorphosis.

The wide range for the environmental reservoir Z_o reflects the great uncertainty underlying possible reservoir sizes. For example, a hypothetical zoospore pool of turnover rate $\mu_\mathrm{Z} = 10^{-3}$, containing a persistent population of 10^3 hosts, each one infected with 10^5 zoospores, each of which releases 10 zoospores per day, will contain 10^{12} zoospores at equilibrium. We refer to section 4.2 for an estimate of plausible transmission rates β_A, β_T.

The range of tadpole lifetimes, τ_m, is based on the life cycle of *R. muscosa* [20] and *R. sylvatica* [51]. The considered host carrying capacities K_A, K_T and survivorships $\sigma_\mathrm{A}, \sigma_\mathrm{T}$ cover typical ranges of observed, pre-exposure population sizes [52, 53, 51, 54, 11]. The range of considered host fecundities r covers estimates for *R. aurora aurora* by Licht [52] and for *R. sylvatica* by Berven [55].

5.2 Parameter sampling

Parameter sampling was performed via Monte Carlo integration over the considered parameter domain [56]. Unless indicated otherwise, all parameters were sampled within the ranges given by table 1 in the main article, at a sample size of 10^4. For each parameter or parameter pair, the functional dependence of the probability of extinction ($\mathcal{P}_\mathrm{ex}$), *Bd* clearance ($\mathcal{P}_\mathrm{cl}$) and *Bd* persistence ($\mathcal{P}_\mathrm{per}$) was estimated by averaging over all sampled values of all the other parameters. This procedure reflects

Table 1: Parameter values used in numerical simulations shown in the main article ('A') and the supplement ('S'). Unless stated otherwise, $Z_o = 0$ (no external reservoir), $\mu_{\mathrm{S,A}} = \mu_{\mathrm{S,T}} = 0.01$ d^{-1}, $\lambda_{\mathrm{A}} = \lambda_{\mathrm{T}} = 0$, $b = 0$ (constant transmission rates), $\varphi = 0$, $\eta_{\mathrm{A}} = \eta_{\mathrm{T}} = 2$ d^{-1}, $\mathcal{T}_{\mathrm{A}} = 10^3$, $\mathcal{T}_{\mathrm{T}} = \mathcal{F}_{\mathrm{T}}$, $S_{\mathrm{T,max}} = \mathcal{F}_{\mathrm{T}} - 1$ (tadpoles tolerate *Bd*), $\mathcal{T}_{\mathrm{m}} = \mathcal{T}_{\mathrm{br}} = 10^6$ (metamorphosis not affected by *Bd*), $\tau_{\mathrm{m}} = Y$, $r = 100$, $\tau_{\mathrm{br}} = 60$ d, $\sigma_{\mathrm{A}} = 0.5$, $\sigma_{\mathrm{T}} = 0.05$, $K_{\mathrm{A}} = 100$, $K_{\mathrm{T}} = 200$, $f_{\mathrm{A}} = f_{\mathrm{T}} = 0.2$.

Fig.	Parameters
A.2(a,b)	$\mu_{\mathrm{Z}} = 1$ d^{-1}, $\mu_{\mathrm{S,A}} = \mu_{\mathrm{S,T}} = 0.2$ d^{-1}, $\overline{\beta}_{\mathrm{A}} = \overline{\beta}_{\mathrm{T}} = 0.001$ d^{-1}, $\tau_{\mathrm{br}} = Y/2$.
A.2(c,d)	$\mathcal{T}_{\mathrm{T}} = 500$, $S_{\mathrm{T,max}} = \mathcal{F}_{\mathrm{T}}$, otherwise as (a,b).
A.3(a)	$\mu_{\mathrm{Z}} = 0.1$ d^{-1}, $\overline{\beta}_{\mathrm{A}} = \overline{\beta}_{\mathrm{T}} = 0.0001$ d^{-1}.
A.3(b)	$\mathcal{T}_{\mathrm{T}} = 10^3$, $S_{\mathrm{T,max}} = \mathcal{F}_{\mathrm{T}}$, otherwise as in (a).
S.2(a,b)	$\mu_{\mathrm{Z}} = 1$ d^{-1}, $\mu_{\mathrm{S,A}} = \mu_{\mathrm{S,T}} = 0.2$ d^{-1}, $\overline{\beta}_{\mathrm{A}} = \overline{\beta}_{\mathrm{T}} = 0.000001$ d^{-1}, $\tau_{\mathrm{br}} = Y/2$, $\sigma_{\mathrm{T}} = 0.2$, $K_{\mathrm{T}} = 2000$.
S.2(c,d)	$\mathcal{T}_{\mathrm{T}} = 500$, $S_{\mathrm{T,max}} = \mathcal{F}_{\mathrm{T}}$, otherwise as (a,b).
S.3(a)	$\mu_{\mathrm{Z}} = 0.1$ d^{-1}, $\overline{\beta}_{\mathrm{A}} = \overline{\beta}_{\mathrm{T}} = 10^{-7}$ d^{-1}, $\sigma_{\mathrm{T}} = 0.2$, $K_{\mathrm{T}} = 2000$.
S.3(b)	$\mathcal{T}_{\mathrm{T}} = 10^3$, $S_{\mathrm{T,max}} = \mathcal{F}_{\mathrm{T}}$, otherwise as in (a).

the idea that, in nature, no two ecosystems are perfectly identical and trends along a certain covariate are always *blurred* by the influence of many other covariates. Simulations started with a healthy population, to which an infected adult is introduced after 1.5 years, as described in the introduction of section 5. Simulations ran up to ten years, or until host extinction. The parameters r, Z_o, μ_{Z}, $\mu_{\mathrm{S,A}}$, $\mu_{\mathrm{S,T}}$, K_{A}, K_{T}, $\overline{\beta}_{\mathrm{A}}$, $\overline{\beta}_{\mathrm{T}}$, $\mathcal{T}_{\mathrm{A}}$, $\mathcal{T}_{\mathrm{T}}$, $\mathcal{T}_{\mathrm{m}}$, r were sampled uniformly on a logarithmic scale (*log-uniformly*), all others on a linear scale (*linear-uniformly*).

The basic reproduction quotient Q_o, given by (19), was estimated for every sampled parameter tuple after approximating $\overline{N}_s \approx K_s$, $\overline{R}_{\mathrm{A}} \approx \frac{K_{\mathrm{T}}}{K_{\mathrm{A}}} \frac{\sigma_{\mathrm{m}}(0)}{\tau_{\mathrm{m}}}$ and $\overline{R}_{\mathrm{T}} \approx \frac{K_{\mathrm{A}}}{K_{\mathrm{T}}} \frac{r}{Y}$. Note that formula (19) is only valid if $\overline{R}_s - \lambda_s > 0$ for all life stages s, so that the statistics on Q_o are restricted to these cases. Finally, we mention that because of the condition that the coefficients c_{A}, c_{T}, given in (9), be positive, the valid parameter domain is not rectangular.

The risk effect of any given model parameter X, which varies in the range $[X_{\min}, X_{\max}]$, was defined as follows: For any fixed value x of X, let $\mathcal{P}_{\mathrm{ex}}(x)$ be the probability of extinction due to a *Bd* exposure as described above, provided that all other parameters are sampled linear-uniformly (or log-uniformly) in their considered range. Let $y = Ax + B$ be the simple linear regression line to $y = \mathcal{P}_{\mathrm{ex}}(x)$ with slope A and intercept B. Then the **risk effect** of X is given by the dimensionless value $A \cdot (X_{\max} - X_{\min})$. We estimated the latter based on the estimate of A for the data obtained through our Monte Carlo simulations. Note that the risk effect depends on the range of the particular parameter as well as the ranges of all other sampled parameters.

5.3 Stochastic host mortalities

To include stochastic mortalities, we replaced the base mortalities $\mu_s(0)$ (where $s \in \{\mathrm{A}, \mathrm{T}\}$) with independent, random fatal events occurring at Poissonian rates $\widetilde{\mu}_s \geq \mu_s(0)$. These events were fatal to a Binomially distributed number of individuals with probability $f_s = \mu_s(0)/\widetilde{\mu}_s$. More precisely, at each time step dt, a disturbance was introduced to the host population at probability $dt \cdot \widetilde{\mu}_s$. In the event of such a disturbance, the total number k_s of killed hosts in a particular life stage s was chosen randomly, according to a binomial distribution of $\lfloor N_s \rfloor$ trials and probability of success f_s. Each DOI bin was then decreased by the factor k_s/N_s. Hence, modifying $\widetilde{\mu}_s$ differentiated between *few but strong* (high f_s) and *many but weak* (low f_s) disturbances, while keeping the expected base mortality fixed. The density-dependent part of $\mu_s(\mathbf{N})$, given in (5), was left unchanged. In the limit $f_s \to 0$, the deterministic version (5) is retrieved. If not stated otherwise, all reported results refer to the case $f_{\mathrm{A}} = f_{\mathrm{T}} = 0.2$.

References

1. Lampo, M., Celsa, S. J., Rodríguez-Contreras, A., Rojas-Runjaic, F. & García, C. Z. 2012 High turnover rates in remnant populations of the harlequin frog *Atelopus cruciger* (*Bufonidae*): Low risk of extinction? *Biotropica* **44**, 420–426. (doi:10.1111/j.1744-7429.2011.00830.x).

2. Rachowicz, L. J., Vredenburg, V. T. *et al.* 2004 Transmission of *Batrachochytrium dendrobatidis* within and between amphibian life stages. *Dis. Aquat. Org.* **61**, 75–83.

3. Rachowicz, L. J., Knapp, R. A., Morgan, J. A., Stice, M. J., Vredenburg, V. T., Parker, J. M. & Briggs, C. J. 2006 Emerging infectious disease as a proximate cause of amphibian mass mortality. *Ecology* **87**, 1671–1683.

4. Garner, T. W., Walker, S., Bosch, J., Leech, S., Marcus Rowcliffe, J., Cunningham, A. A. & Fisher, M. C. 2009 Life history tradeoffs influence mortality associated with the amphibian pathogen *Batrachochytrium dendrobatidis*. *Oikos* **118**, 783–791. (doi:10.1111/j.1600-0706.2008.17202.x).

5. Blaustein, A. R., Romansic, J. M., Scheessele, E. A., Han, B. A., Pessier, A. P. & Longcore, J. E. 2005 Interspecific variation in susceptibility of frog tadpoles to the pathogenic fungus *Batrachochytrium dendrobatidis*. *Conserv. Biol.* **19**, 1460–1468. (doi:10.1111/j.1523-1739.2005.00195.x).

6. Kilpatrick, A. M., Briggs, C. J. & Daszak, P. 2010 The ecology and impact of chytridiomycosis: An emerging disease of amphibians. *Trends Ecol. Evol.* **25**, 109–118. (doi:10.1016/j.tree.2009.07.011).

7. Stockwell, M. P., Clulow, J. & Mahony, M. J. 2010 Host species determines whether infection load increases beyond disease-causing thresholds following exposure to the

amphibian chytrid fungus. *Anim. Conserv.* **13**, 62–71. (doi:10.1111/j.1469-1795.2010.00407.x).

8. Brannelly, L. A., Chatfield, M. W. & Richards-Zawacki, C. L. 2012 Field and laboratory studies of the susceptibility of the green treefrog (*Hyla cinerea*) to *Batrachochytrium dendrobatidis* infection. *PLoS ONE* **7**, e38473.

9. Gervasi, S., Gondhalekar, C., Olson, D. H. & Blaustein, A. R. 2013 Host identity matters in the amphibian *Batrachochytrium dendrobatidis* system: Fine-scale patterns of variation in responses to a multi-host pathogen. *PLoS ONE* **8**, e54490.

10. Carey, C., Bruzgul, J. E., Livo, L. J., Walling, M. L., Kuehl, K. A., Dixon, B. F., Pessier, A. P., Alford, R. A. & Rogers, K. B. 2006 Experimental exposures of boreal toads (*Bufo boreas*) to a pathogenic chytrid fungus (*Batrachochytrium dendrobatidis*). *EcoHealth* **3**, 5–21.

11. Vredenburg, V. T., Knapp, R. A., Tunstall, T. S. & Briggs, C. J. 2010 Dynamics of an emerging disease drive large-scale amphibian population extinctions. *Proc. Natl. Acad. Sci. USA* **107**, 9689–9694. (doi:10.1073/pnas.0914111107).

12. Cashins, S. D., Grogan, L. F., McFadden, M., Hunter, D., Harlow, P. S., Berger, L. & Skerratt, L. F. 2013 Prior infection does not improve survival against the amphibian disease chytridiomycosis. *PLoS ONE* **8**, e56747. (doi:10.1371/journal.pone.0056747).

13. Murray, K. A., Skerratt, L. F., Speare, R. & McCallum, H. 2009 Impact and dynamics of disease in species threatened by the amphibian chytrid fungus, *Batrachochytrium dendrobatidis*. *Conserv. Biol.* **23**, 1242–1252. (doi:10.1111/j.1523-1739.2009.01211.x).

14. Ribas, L., Li, M.-S., Doddington, B. J., Robert, J., Seidel, J. A., Kroll, J. S., Zimmerman, L. B., Grassly, N. C., Garner, T. W. & Fisher, M. C. 2009 Expression profiling the temperature-dependent amphibian response to infection by *Batrachochytrium dendrobatidis*. *PLoS ONE* **4**, e8408.

15. Rollins-Smith, L. A., Doersam, J. K., Longcore, J. E., Taylor, S. K., Shamblin, J. C., Carey, C. & Zasloff, M. A. 2002 Antimicrobial peptide defenses against pathogens associated with global amphibian declines. *Dev. Comp. Immunol.* **26**, 63–72.

16. Rollins-Smith, L. A., Woodhams, D. C., Reinert, L. K., Vredenburg, V. T., Briggs, C. J., Nielsen, P. F. & Michael Conlon, J. 2006 Antimicrobial peptide defenses of the mountain yellow-legged frog (*Rana muscosa*). *Dev. Comp. Immunol.* **30**, 831–842.

17. Woodhams, D., Ardipradja, K., Alford, R., Marantelli, G., Reinert, L. & Rollins-Smith, L. 2007 Resistance to chytridiomycosis varies among amphibian species and is correlated with skin peptide defenses. *Anim. Conserv.* **10**, 409–417.

18. Kriger, K. M. & Hero, J.-M. 2006 Survivorship in wild frogs infected with chytridiomycosis. *EcoHealth* **3**, 171–177.

19. Berger, L., Hyatt, A. D., Speare, R. & Longcore, J. E. 2005 Life cycle stages of the amphibian chytrid *Batrachochytrium dendrobatidis*. *Dis. Aquat. Org.* **68**, 51–63. (doi:10.3354/dao068051).

20. Briggs, C. J., Knapp, R. A. & Vredenburg, V. T. 2010 Enzootic and epizootic dynamics of the chytrid fungal pathogen of amphibians. *Proc. Natl. Acad. Sci. USA* **107**, 9695–9700. (doi:10.1073/pnas.0912886107).

21. Brem, F. M. & Lips, K. R. 2008 *Batrachochytrium dendrobatidis* infection patterns among panamanian amphibian species, habitats and elevations during epizootic and enzootic stages. *Dis. Aquat. Org.* **81**, 189. (doi:10.3354/dao01960).

22. Mitchell, K. M., Churcher, T. S., Garner, T. W. & Fisher, M. C. 2008 Persistence of the emerging pathogen *Batrachochytrium dendrobatidis* outside the amphibian host greatly increases the probability of host extinction. *Proc. R. Soc. B: Biol. Sci.* **275**, 329–334. (doi:10.1098/rspb.2007.1356).

23. Longcore, J. E., Pessier, A. P. & Nichols, D. K. 1999 *Batrachochytrium dendrobatidis* gen. et sp. nov., a chytrid pathogenic to amphibians. *Mycologia* **91**, 219–227.

24. Piotrowski, J. S., Annis, S. L. & Longcore, J. E. 2004 Physiology of *Batrachochytrium dendrobatidis*, a chytrid pathogen of amphibians. *Mycologia* **96**, 9–15.

25. Woodhams, D. C., Alford, R. A., Briggs, C. J., Johnson, M. & Rollins-Smith, L. A. 2008 Life-history trade-offs influence disease in changing climates: strategies of an amphibian pathogen. *Ecology* **89**, 1627–1639. (doi:10.1890/06-1842.1).

26. Retallick, R. W., McCallum, H. & Speare, R. 2004 Endemic infection of the amphibian chytrid fungus in a frog community post-decline. *PLoS Biol.* **2**, e351. (doi:10.1371/journal.pbio.0020351).

27. Berger, L., Speare, R., Hines, H., Marantelli, G., Hyatt, A., McDonald, K. R., Skerratt, L., Olsen, V., Clarke, J., Gillespie, G. *et al.* 2004 Effect of season and temperature on mortality in amphibians due to chytridiomycosis. *Aust. Vet. J.* **82**, 434–439.

28. Mardia, K. & Jupp, P. 2000 *Directional Statistics*. Wiley Series in Probability and Statistics. Wiley. ISBN 9780471953333.

29. Verhulst, P. F. 1838 Notice sur la loi que la populations suit dans son accroissement. *Corresp. Math. Phys.* **10**, 113–121.

30. Altizer, S., Dobson, A., Hosseini, P., Hudson, P., Pascual, M. & Rohani, P. 2006 Seasonality and the dynamics of infectious diseases. *Ecol. Lett.* **9**, 467–484.

31. Anderson, R. M. & May, R. M. 1978 Regulation and stability of host-parasite population interactions: I. Regulatory processes. *J. Anim. Ecol.* pp. 219–247.

32. May, R. M. & Anderson, R. M. 1978 Regulation and stability of host-parasite population interactions: II. Destabilizing processes. *J. Anim. Ecol.* pp. 249–267.

33. Roberts, M. G., Smith, G. & Grenfell, B. T. 1995 *Mathematical Models for Macroparasites of Wildlife*, pp. 177–208. Publications of the Newton Institute. Cambridge University Press.

34. Meiss, J. 2007 *Differential Dynamical Systems*. Number v. 1 in Monographs on Mathematical Modeling and Computation. Society for Industrial and Applied Mathematics. ISBN 9780898716351.

35. Betounes, D. 2010 *Differential Equations: Theory and Applications: With Maple*. Springer London, Limited. ISBN 9781441911636.

36. Engel, K. & Nagel, R. 2000 *One-parameter semigroups for linear evolution equations*. Springer.

37. Eisner, T. 2010 *Stability of operators and operator semigroups*. Operator Theory: Advances and Applications. Birkhäuser. ISBN 9783034601948.

38. Bellman, R. 1943 The stability of solutions of linear differential equations. *Duke. Math. J.* **10**, 643–647. (doi:10.1215/S0012-7094-43-01059-2).

39. Diekmann, O. & Heesterbeek, J. 2000 *Mathematical Epidemiology of Infectious Diseases: Model Building, Analysis and Interpretation*. Wiley Series in Mathematical & Computational Biology. Wiley. ISBN 9780471492412.

40. Diekmann, O., Heesterbeek, J. & Metz, J. 1990 On the definition and the computation of the basic reproduction ratio R_o in models for infectious diseases in heterogeneous populations. *J. Math. Biol.* **28**, 365–382.

41. Van den Driessche, P. & Watmough, J. 2002 Reproduction numbers and sub-threshold endemic equilibria for compartmental models of disease transmission. *Math. Biosci.* **180**, 29–48.

42. Hinch, E. 1991 *Perturbation Methods*. Cambridge Texts in Applied Mathematics. Cambridge University Press. ISBN 9780521378970.

43. Márquez, M., Nava-González, F., Sánchez, D., Calcagno, M. & Lampo, M. 2010 Immmunological clearance of *Batrachochytrium dendrobatidis* infection at a pathogen-optimal temperature in the hylid frog *Hypsiboas crepitans*. *EcoHealth* **7**, 380–388.

44. Black, A. J. & McKane, A. J. 2012 Stochastic formulation of ecological models and their applications. *Trends Ecol. Evol.* **27**, 337 – 345. ISSN 0169-5347. (doi:10.1016/j.tree.2012.01.014).

45. Begon, M., Bennett, M., Bowers, R., French, N., Hazel, S., Turner, J. *et al.* 2002 A clarification of transmission terms in host-microparasite models: numbers, densities and areas. *Epidemiol. Infect.* **129**, 147–153.

46. Rachowicz, L. J. & Briggs, C. J. 2007 Quantifying the disease transmission function: effects of density on *Batrachochytrium dendrobatidis* transmission in the mountain yellow-legged frog *Rana muscosa*. *J. Anim. Ecol.* **76**, 711–721.

47. Hoffman, J. & Frankel, S. 2001 *Numerical Methods for Engineers and Scientists, Second Edition,*. Taylor & Francis. ISBN 9780824704438.

48. Johnson, M. L. & Speare, R. 2003 Survival of *Batrachochytrium dendrobatidis* in water: quarantine and disease control implications. *Emerg. Infect. Dis.* **9**, 922. (doi:10.3201/eid0908.030145).

49. Hyatt, A., Boyle, D., Olsen, V., Boyle, D., Berger, L., Obendorf, D., Dalton, A., Kriger, K., Hero, M., Hines, H. *et al.* 2007 Diagnostic assays and sampling protocols for the detection of *Batrachochytrium dendrobatidis*. *Dis. Aquat. Org.* **73**, 175–192. (doi:10.3354/dao073175).

50. Beldomenico, P. M. & Begon, M. 2010 Disease spread, susceptibility and infection intensity: vicious circles? *Trends Ecol. Evol.* **25**, 21–27.

51. Berven, K. A. 1990 Factors affecting population fluctuations in larval and adult stages of the wood frog (*Rana sylvatica*). *Ecology* **71**, 1599–1608.

52. Licht, L. E. 1974 Survival of embryos, tadpoles, and adults of the frogs *Rana aurora aurora* and *Rana pretiosa pretiosa* sympatric in southwestern British Columbia. *Can. J. Zool.* **52**, 613–627.

53. Elmberg, J. 1990 Long-term survival, length of breeding season, and operational sex ratio in a boreal population of common frogs, *Rana temporaria* L. *Can. J. Zool.* **68**, 121–127.

54. Laurance, W. F., McDonald, K. R. & Speare, R. 1996 Epidemic disease and the catastrophic decline of Australian rain forest frogs. *Conserv. Biol.* **10**, 406–413.

55. Berven, K. A. 1988 Factors affecting variation in reproductive traits within a population of wood frogs (*Rana sylvatica*). *Copeia* pp. 605–615.

56. Kroese, D., Taimre, T. & Botev, Z. 2011 *Handbook of Monte Carlo Methods*. Wiley Series in Probability and Statistics. Wiley.